"Vibration sensitive afferents rather than spatial acuity determine tactile roughness discrimineration"

Libouton, Xavier

Abstract

The human hand is a wondrous instrument that serves us extremely well in a multitude of applications. In every day life, we frequently explore surfaces with our fingertips to estimate different aspects of their physics. We use our hands to identify objects and surface textures with high accuracy. Tactile information tells a person how much force to use when grasping objects, which range from rigid, such as a steel marble to delicate, such as a tomato. Researchers are currently working on developing prosthetic systems that incorporate touch-sensitive feedback. Understanding the neurobiology of roughness perception could be revolutionary to the utility of hand prosthetics. In this thesis, a psychophysical method to estimate roughness threshold with the sandpaper set was developed and validated. Secondarily, we examined the relative contribution of remote mechanoreceptors to perception of roughness versus spatial acuity in various conditions that affect innervation of the index finger d...

Document type : *Thèse (Dissertation)*

VIBRATION SENSITIVE AFFERENTS RATHER THAN SPATIAL ACUITY DETERMINE TACTILE ROUGHNESS DISCRIMINATION.

By Xavier Libouton

Thesis submitted in fulfillment of the requirements for the degree of «Docteur en Sciences Médicales »

May 2015

Remerciements

La réalisation de cette thèse fut pour moi l'occasion de rencontrer de nombreuses personnes. Ce travail est le fruit de l'ensemble de ces rencontres, de ces interactions.

Mes premiers remerciements iront à l'ensemble des personnes que je vais certainement et involontairement oublier de citer. J'espère qu'elles m'en excuseront. Je vous témoigne néanmoins toute ma gratitude.

Ensuite, je voudrais remercier en premier trois personnes fondamentales dans l'accomplissement de ce travail. Jean-Louis, en tant que responsable du laboratoire, tu nous permets de travailler dans un magnifique cadre de travail où l'échange, la collaboration, la critique positive ne sont pas que des mots. En tant que promoteur de ma thèse, tu m'as soutenu en permanence, tu m'as canalisé quand il le fallait et tu y es pour beaucoup si ce travail a pu aboutir. En tant que personne, comment oublier ces heures de discussions à refaire le monde, à voyager aux 4 coins de l'Europe pour le projet Nanobiotact…à chercher notre chemin légèrement égaré au fin fond d'une forêt munichoise. Pour tout cela et le reste, reçois mes plus profonds remerciements.

Léon, la force tranquille, l'homme de l'ombre, tout au long de ce parcours, tu n'as cessé de m'encourager, de suggérer, d'encadrer, de relire l'ensemble de ce travail. Tu es toujours disponible. Ta connaissance scientifique est infinie et tu nous la fais partager avec une telle humilité que cela force le respect. Sincèrement, Merci !

Olivier, notre rencontre date d'il y a maintenant tant d'années. Tu as été le premier à me suggérer la réalisation d'une thèse. Tu es l'instigateur de ma rencontre avec Jean-Louis. En tant que co-promoteur, tu as encadré au mieux ce travail malgré une activité clinique débordante. Maintenant, bien qu'ayant des personnalités différentes, nous formons quotidiennement un binôme chirurgical complémentaire basé sur le respect et la symbiose. Jamais avare d'un conseil, tu me cadres parfaitement. Tu n'hésites jamais à me communiquer ta connaissance chirurgicale encyclopédique. Quel plaisir de pouvoir travailler dans de telles conditions. Merci !

Je remercie aussi l'ensemble du Jury de cette thèse. Merci de me consacrer de votre temps précieux pour permettre l'accomplissement de ce travail. Merci pour vos remarques et suggestions qui ont permis à ce manuscrit de devenir ce qu'il est.

Je voudrais aussi remercier l'ensemble du feu laboratoire READ pour toutes vos richesses. Merci à Fred, Delphine, Yannick, Olivier, Damienne, Céline, Olivier, Laure, Christine, Christian, Charles, André, etc. Un merci aussi tout particulier à Thibaut qui est devenu un ami.

J'en profite aussi pour remercier l'ensemble du la structure Naniobact qui a aussi grandement contribué à ce travail.

Un merci tout particulier à mes parents qui ont toujours fait tout ce qu'ils pouvaient pour nous permettre d'avoir accès au meilleur possible.

Enfin, je conclurai ce petit mot en remerciant deux personnes et bientôt trois qui me sont les plus chères. Véronique, tu as débarqué dans ma vie, tu m'as redonné confiance. Ce travail n'aurait sans doute pas été mené à terme sans ta présence. Juliette, tous les jours, tu me donnes cette envie de se dépasser. Toutes les deux par votre présence, vous me transmettez cette force qui permet de rendre plus joyeux le quotidien. Je vous aime profondément. Merci !

Jury

Chair:

Prof. Bénédicte Schepens (Institut de neuroscience, UCL, Belgium)

Supervisors:

Prof. Jean-Louis Thonnard (Institut de neuroscience, UCL, Belgium)

Prof. Olivier Barbier (Département d'orthopédie et de traumatologie, UCL, Belgium)

Members:

Prof. Frédéric Schuind (Département d'orthopédie et de traumatologie, ULB, Erasme)

Prof. Léon Plaghki (Institut de neuroscience, UCL, Belgium)

Prof. Philippe Lefèvre (Institut de neuroscience, UCL, Belgium)

Table of Contents:

Chapter 1: Introduction and background

The human hand is a wondrous instrument that serves us extremely well in a multitude of applications. We use our hands to identify objects and surface textures with high accuracy. We demonstrate remarkable manual dexterity when reaching for, grasping, and manipulating objects. Furthermore, the hand is a powerful tool of communication.

Lederman and Jones (Jones and Lederman, 2006) conceptualize hand function along a sensory-motor continuum within which they delineate four categories: tactile sensing, active haptic sensing, prehension, and non-prehensile skilled movements. In tactile sensing, the hand acts passively and moves relative to stimuli to affect contact. It provides some information about surface texture and thermal conductivity, especially when an object or surface is moved across the skin. Meanwhile active haptic sensing requires voluntary hand movement around an object or over a surface; it is preferred for object identification and extraction of information about an object's properties. Prehension refers to activities in which the hand reaches to grasp an object. Non-prehensile skilled movements are a diverse class of behavioral movements that may involve all of the hand's fingers and both hands, such as typing and sign language.

Though tactile perception is considered to be one of the five traditional senses, the impression of touch is formed from several input modalities. The somatosensory system receives input through a variety of receptor types—each of which transduces a specific form of energy into action potentials—and their associated processing centers in the central nervous system (CNS). Receptor signals are transmitted via peripheral sensory nerves through spinal cord tracts to the brain. The processing centers within the somatosensory system produce the sensations of touch, temperature, proprioception, and nociception. The skin and its embedded mechanoreceptors serve an especially important role in gathering information about the external world through the sense of touch (Scheibert et al., 2009). Information about the external world is analyzed in distinct processing streams specialized for particular sensory systems. The system filters and shapes incoming tactile information. Within the somatosensory system, the multiple subsystems are each attuned to gathering particular aspects of information. Nociceptors, mechanoreceptors, proprioceptors, and cutaneous mechanoreceptors

transduce different stimulus properties and channel their information into separate, parallel streams.

Somatosensory perception provides important feedback to ongoing hand movements. Modern prosthetic hands are able to mimic a cinematic model of global hand movements in the absence of somatosensory perception, but further improvements in technology are needed to yield full functionality. At the 2009 IEEE annual conference, Maria Carrozza described the current state of hand prosthetics as follows:

> *The design and development of a prosthetic artificial hand should aim as much as possible at replacing both functionality and cosmetic appearance of the natural hand lost by the amputee. Surveys on using commercial prosthetic hands reveal that 30 to 50 percent of upper-extremity amputees do not use their prosthetic hand regularly. The main factors for this are low functionality and controllability, poor cosmetic appearance, and an unnatural control system, which make the hand to be felt as an external device that is not part of the subject's body scheme.*

Hence, it is of utmost importance that we better understand how the human somatosensory system functions so that we can design biomechatronic devices that mimic and restore human abilities more effectively (Tabot et al., 2013). This goal is the underlying motivation for my work in the field of roughness perception.

Our current understanding of roughness perception, from the finger pad to the brain, is reviewed in this chapter, including descriptions of the skin structures and functions relevant to the four subclasses that together define the hand-function continuum. This work focuses specifically on those aspects important for roughness perception. Thus, skin structures not involved in roughness perceptions, such as thermoreceptors and nociceptors, are not reviewed here.

1- The skin

Human skin is a biologically complex material consisting of three principal tissue layers: the epidermis, dermis, and hypodermis (subcutaneous fat layer) (see fig. 1)(Young, 2006). The skin serves as a protective interface between the internal body and the external environment (Mountcastle, 2005).The epidermis and dermis tissue layers are important for somatosensory function and therefore described in detail below.

The superficial, avascular epidermis consists of 4–5 layers of epithelial cells resting upon a basement membrane. Within the epidermis there are multiple cell types including keratinocytes, which provide structure, melanocytes, which produce pigment, Merkel cells, which contain mechanoreceptors, and Langerhans' cells, which play a role in immune defense. The chief function of keratinocytes is the production of keratin, a tough fibrous protein that confers sturdiness and fortification. The basement membrane is attached firmly to the underlying dermis. It is a single layer of cuboidal keratinocytes with interspersed melanocytes and Merkel cells. The cells in this layer are highly mitotic.

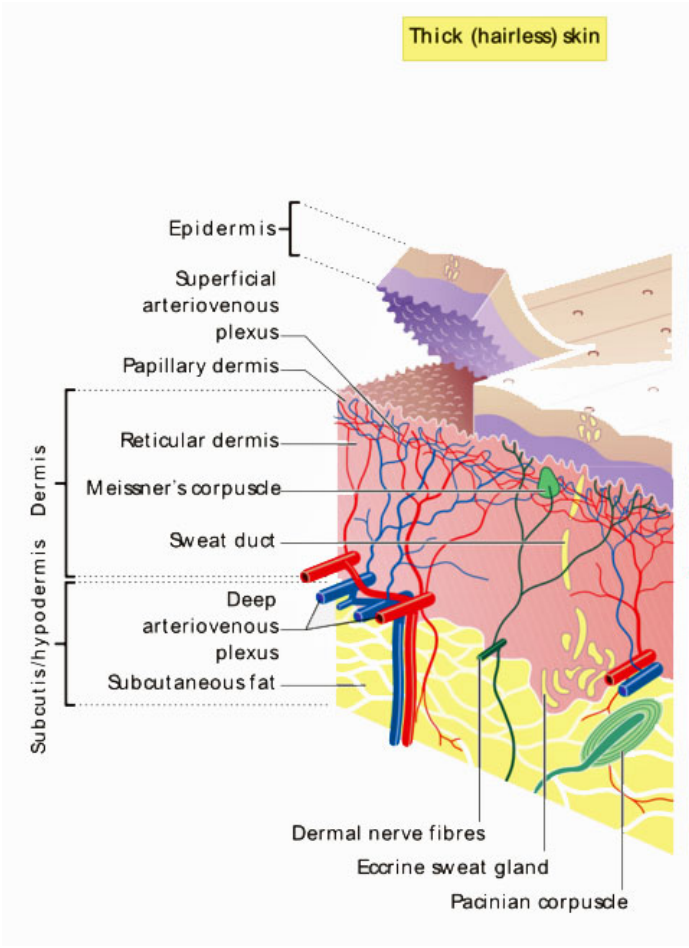

Figure 1: Typical histological structure of the glabrous skin fingertip

The deep, vascular dermis consists mainly of fibrous connective tissue and is enriched with blood vessels. It includes two sublayers, namely the relatively superficial papillary dermis and the reticular dermis beneath the papillary dermis. The papillary dermis consists of loose connective tissue and contains multiple sensory receptors. It interdigitates with, and thus is attached

firmly to, the epidermis. The reticular dermis consists of interconnected collagen and elastin fibers in a semi-fluid structure.

1.1 Cutaneous innervation

The skin is densely innervated, which enables it to serve multiple functions, including the perception of touch, warmth, cold, and pain. The distribution and density of specific types of nerve endings differ between various body regions and between different parts of the skin. Areas with very dense nerve endings include the fingerpads, lips, and genitalia (Lauria et al., 1999). It should be noted that other afferent units beyond the skin, including receptors in the joints and muscles, may also play very important roles in tactile sensibility in a broader sense.

Cutaneous sensory neurons employ different specialized transducers to mediate highly specific sensory functions. Changes in thermal or mechanical energy in the skin are perceived as specific sensations. Thermal or mechanical change is represented by the transfer of energy into the skin and transduction by a specific type of sensory axonal terminal. Some axon terminals are polymodal, meaning that they respond to more than one type of energy. Thermal senses and light touch are each produced by transduction of a single form of energy, whereas pain can be produced by a change in either thermal or mechanical energy that is associated with potential tissue damage. Technical innovations in molecular biology have revealed a tremendous diversity of ionotropic and metabotropic receptors, channels, and neurotransmitters. Cutaneous neurites and receptors are now visualized commonly by immunohistochemical labeling with antibodies against ubiquitin carboxy-terminal hydrolase L1 (UCHL1), also known as protein gene product 9.5. UCHL1 is an enzyme that is located exclusively and ubiquitously in neurons. UCHL1 labeling has revealed that there are far more cutaneous nerve endings than previously thought (O. Johansson et al., 1999; Wilkinson et al., 1989).

The major function of somatic cutaneous axons is the transmission of sensory information. Localization of a stimulus (i.e. which part of the body is being simulated) is resolved based on the rigid somatotopic organization of the neurons and synapses of the somatosensory pathways from the skin, through the spinal cord or brain stem, to the somatosensory cortex.

Sensory axons are classified morphologically as myelinated (A-fibers) or unmyelinated (C-fibers). Myelination increases axonal conduction velocity. A-fibers are further subdivided according to axonal diameter, with Aα sensory axons having diameters of approximating 10 μm and Aδ sensory axons having diameters wider than 1 μm. Fine Aα fibers are sometimes inappropriately denoted as Aβ fibers (Burgess and Perl, 1973). Unmyelinated C-fibers, which have diameters of up to 1.5 μm, conduct at a rate of about 1 m/s, far slower than the 40–100-m/s conduction rates of thickly myelinated A-fibers. Sensory axons frequently enter the epidermis either to terminate as free nerve endings or to associate with histological structures like Merkel cells or Pacinian corpuscles(Munger and Ide, 1988).

Electrophysiological recordings can be obtained from single cutaneous axons while defined stimuli are applied to the axon's cutaneous receptive field with ultra-microneurography (Vallbo and Hagbarth, 1968). Employing ultra-microneurography and anatomical studies, Vallbo and colleagues (Vallbo and R. S. Johansson, 1984) found strong, albeit indirect, evidence suggesting that all of the tactile units in the glabrous skin of the hand have Aα fibers, with the Aδ and unmyelinated C fibers belonging to nociceptive and thermosensitive units. They defined the *tactile unit* as a primary afferent neuron whose sensory endings are primarily responsive to light skin deformations and are located mostly in the dermis. The functional properties of specific types of cutaneous neurons can also be characterized. For example, some tactile units fire mostly at the onset of a continuous stimulus (i.e. rapidly adapting), while others maintain firing throughout a prolonged stimulus (i.e. slowly adapting). Sensory signals undergo tremendous modulation and integration in the CNS.

1.2 Mechanoreception

It has been estimated that approximately 17,000 tactile units supply the glabrous skin of each hand (R. S. Johansson and Vallbo, 1979). These tactile units are of four main types (Vallbo and R. S. Johansson, 1984) (fig.2):

1. Slowly adapting type 1 (SA1) afferents (25%), which terminate in Merkel cells
2. Rapidly adapting type 1 (RA1) afferents (43%), which terminate in Meissner corpuscles

3. Rapidly adapting type 2 (RA2) afferents (13%), which terminate in Pacinian corpuscles

4. Slowly adapting type 2 (SA2) afferents (19%), which are thought to terminate in Ruffini endings.

RA1 and RA2 afferents respond only transiently to sudden, steady indentation, whereas SA1 and SA2 afferents respond to sustained skin deformation with a sustained discharge that declines slowly. The type 1 versus type 2 distinction is based on characteristics of the neurons' receptive fields. Type 1 distinguishes tactile units with a small receptive field and distinct borders, whereas Type 2 refers to units with larger receptive fields and diffuse borders.

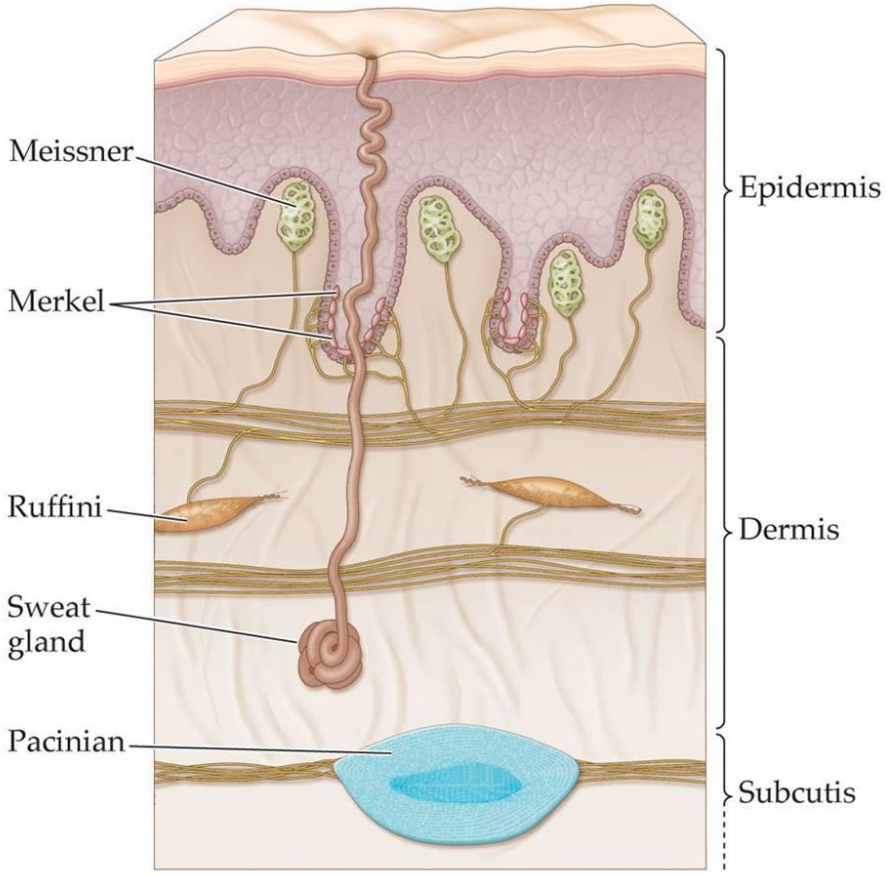

Figure 2: Location of Meissner, Merkel, Pacinian and Ruffini endings

1.2.1 Merkel cells

Since their discovery by Friedrich S. Merkel in 1875 (Lucarz and Brand, 2007), numerous research groups have examined Merkel cells from various body parts of many species using immunohistochemistry and laser confocal microscopy. In mammals, Merkel cells are located in whisker follicles, the hard palate, specialized epithelial structures of the hairy skin called touch domes (Doucet et al., 2013), and glabrous skin surfaces including the palms of the hands and soles of the feet. In glabrous skin (fig.3), they are located in the basal layer of the epidermis in close contact with terminal nerves. They establish synaptic contact with discoid terminals of myelinated axons, which lose their myelin sheath upon entering the epidermis (Halata et al., 2003). Ultrastructural studies have revealed surface lobulations and spine-like protrusions called microvilli on Merkel cells.

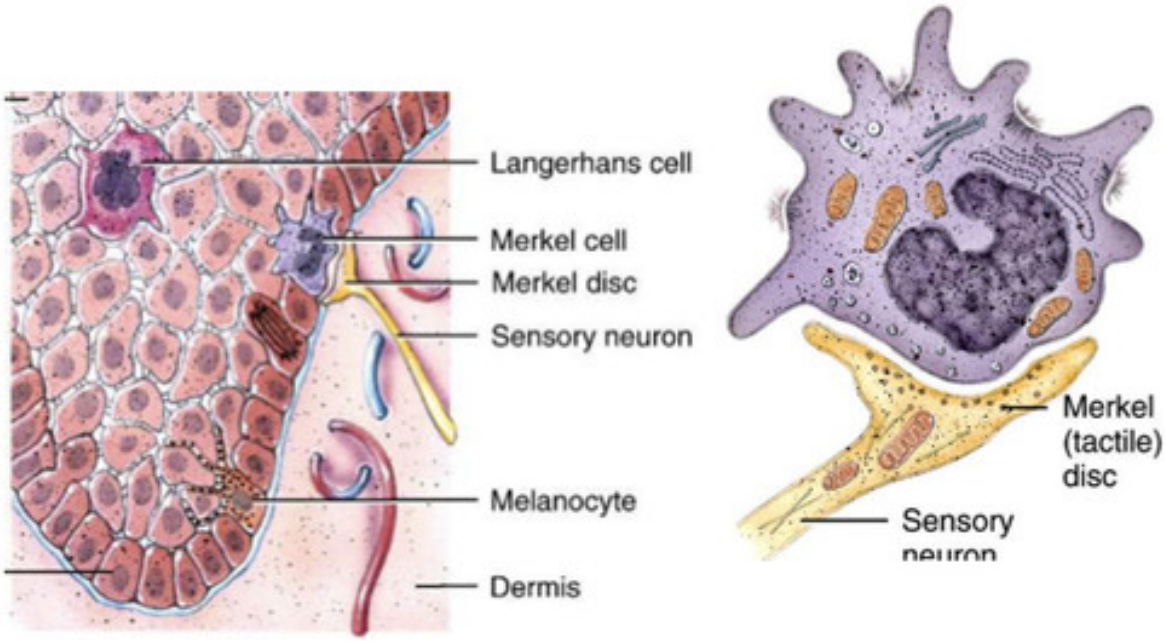

Figure 3: Merkel cell is located in the basal layer of the epidermis and is a highly specialized cell that primarily acts as a slowly adapting mechanoreceptor

Physiologically, Merkel cells are generally regarded as mechanoreceptors that detect tissue deformations with their microvilli and release neurotransmitters to nerve endings as a result(Takahashi-Iwanaga and Abe, 2001). The fingertips are densely innervated with Merkel cell afferents (~ 100 per cm^2)(Johnson, 2001), endowing them with two remarkable response properties (Johnson, 2001): (1) sensitivity to points,

edges, and curvature (Goodwin et al., 1997), and (2) fine spatial resolution. Indeed, an individual SA1 afferent can resolve spatial detail as fine as 0.5 mm. Thus, SA1 afferents can transmit a precise spatial neural image of a tactile stimulus.

Recently, Maricich et al. (Maricich et al., 2009) observed that genetic deletion of Merkel cells caused loss of SAI Aα-fiber responses to mechanical stimulation of the skin, demonstrating that these cells are necessary for receptor function. When they genetically engineered mice that lack Merkel cells (Maricich et al., 2012), they found that the modified mice were not able to detect textured surfaces (rough sandpapers) with their feet. Their findings provide strong evidence that Merkel cell/neurite complexes are essential for texture discrimination involving glabrous skin but not whiskers.

1.2.2 Meissner corpuscles

Initially called Wagner-Meissner corpuscles because they were first described in 1852 by Wagner and Meissner, Meissner corpuscles (as they are now commonly referred to) consist of axon terminals associated with non-neural lamellar cells. The corpuscles are often encapsuled by cells resembling perineural cells (Munger and Ide, 1988) and are trophically dependent on their sensory innervation (Dellon and Munger, 1983). Following nerve transection, the axons are destroyed and their associated lamellae undergo atrophy. They are located in the tips of the dermal papillae, within the dermis but at a minimal distance from the skin surface.

At a physiological level, RA1 afferents associated with Meissner corpuscles innervate the skin more densely than do SA1 afferents, with their densities in the human fingertip being about 150 per cm^2. They are rapidly adapting units with a maximal sensitivity in the range of 40 Hz, well below that of Pacinian corpuscles (Munger and Ide, 1988). When stimulated within their optimal range, Meissner's corpuscle afferents produce action potentials in a nearly perfect one to one relationship with stimulus shifts.

Meissner corpuscles have a receptive field that is 3~5 mm in diameter. They respond to stimuli over the entire receptive field with relative uniformity, and thus are not well-suited for fine spatial resolution. They are insensitive to static skin deformation. But, it appears that their broad, uniform sensitivity enables them to detect slippage between

the skin and an object held in the hand (R. S. Johansson and Westling, 1984; Macefield et al., 1996; Srinivasan et al., 1990). Indeed, because they are able to detect microscopic slips between an object and the skin in a manner that results in reflexive increases in grip force, RA1 afferents could be considered the essential feedback sensors for grip control.

1.2.3 Pacinian corpuscles

Initially described by Vater in 1741 and then rediscovered by Pacini in 1840 (Munger and Ide, 1988), Pacinian corpuscles are the largest sensory corpuscles in the mammalian body. They are usually found in the palmar and plantar aponeurosis, in the genitalia beneath the skin, and in ligaments and joint capsules. They are distributed throughout the palm (about 800) and the finger (about 350) (Johnson, 2001). A peculiarity of the Pacinian system is that it is virtually absent from the lower face. Perhaps the low Pacinian corpuscle sensitivity in the orofacial region prevents the CNS from being overloaded by the large vibrations generated by breathing, talking, and eating.

Pacinian corpuscles have a distinctive appearance under the light microscope consisting of two internal compartments (the inner and outer cores) surrounded by a dense capsule. Each is innervated usually by a single axon in the center of the inner core. Typically, an Aα fiber enters one pole of the corpuscle at which point the myelin sheath ends abruptly and is replaced by the cellular processes of the inner core. This unmyelinated portion of the axon terminates in an expanded tip.

In functional terms, Pacinian corpuscles signal the onset or cessation of compression or vibration transmitted to the body. When stimulated with a vibrating probe, they have maximal sensitivity around 300 Hz (Bolanowski and Zwislocki, 1984). Pacinian corpuscle mechanoreceptors have larger, less defined receptive fields than Meissner's corpuscles, which is suggestive of a relatively poor spatial localization capacity. Interestingly, Brisben et al. (Brisben et al., 1999) reported that Pacinian corpuscles in human hands are tuned to sense the texture of an object or its dimensions indirectly through the use of tools. Additionally, using biomimetic sensors, Scheibert et al. (Scheibert et al., 2009) observed that the normal spacing of fingerprint ridges amplifies vibrations in the ideal detection range of Pacinian corpuscles when scanning across a

finely textured surface (spatial scale < 200 μm). The rapidly adapting properties of Pacinian corpuscles are thought to be due to the outer core. Loewenstein et al. (Loewenstein and Skalak, 1966) reported that dissection of a portion of the outer core changed the adaptive properties of isolated corpuscles. Moreover, Pacinian corpuscles are endowed with remarkable anisotropy. Because compression produces depolarization, rotation of the corpuscle by 90° results in hyperpolarization upon compression.

1.2.4 Ruffini endings

First described by Angelo Ruffini in Siena in 1898, Ruffini endings are corpuscles with an elongated morphological structure and tapered ends. They are quite similar to Golgi tendon organs innervated by proprioceptors (Halata and Munger, 1980). Histologically, the Ruffini ending is usually encased in a capsule of 4–5 layers of perineural cells and contains a core of Schwann cells and collagen. It is innervated by a single large-diameter myelinated axon. The axon loses its myelination at its entry point into the inner core, where it diverges into numerous terminal branches.

The morphological structure of Ruffini endings was first extensively characterized in the hairy skin of the cat by Chambers et al. (Chambers et al., 1972). The species-variant anatomical disbursement of Ruffini endings remains perplexing. SAII responses can be recorded in nerve fibers innervating a tissue with no histologically verifiable Ruffini corpuscles (R. S. Johansson and Vallbo, 1979), (Turnbull and Rasmusson, 1986). Moreover, the skin of the index finger may have only a single Ruffini corpuscle, which is far fewer than would be expected based on physiological recordings (Par et al., 2003).

Physiologically, SAII responses can be differentiated from SAI responses because they usually display some background firing activity when no stimulus is being applied. They also fire at a much more regular rate during their static phase and the maximum frequency of their response is less than that of the SAI response. SAII systems provide information important for the perception of hand conformation and for the perception of forces acting on the hand (Johnson et al., 2000). It appears that they do so by acting primarily as stretch receptors. They have two putative functions: (1) working in combination with RA mechanoreceptors to sense movement of grasped objects; and (2)

working with proprioceptors to localize the positions of the fingers and hand (Johnson, 2001).

2- Biomechanic of the finger pad

Many aspects of both grip function and tactile perception depend on complex frictional interactions occurring in the contact zone of the finger pad. In perceptual tasks such as surface discrimination, the normal force exerted by the finger on the scanned stimulus must be modulated to provoke a controlled slip. Responses elicited from strain-sensitive cutaneous mechanoreceptors at the finger pad as well as from motor control systems that sense length and power based on sensory input from both cutaneous and muscle mechanoreceptors are implicated in the precise control of finger pressure.

Sliding enhance greatly the subjective assessment of the roughness of fine but not coarse textures. Despite the movement of the finger pad over such surfaces causes essentially vibrations, it's reasonable to expect that friction of the finger pad may also play a role in assessing the surface roughness. Skedung et al. (Skedung et al., 2010) found that the subjects reduced the normal force as the coefficient of friction increased for test papers having different roughness. While, correlations with perceived roughness have been found with both the measured roughness and the coefficient of friction as mentioned by Smith et al. (Smith et al., 2010). It emphasizes the importance of friction.

In tactile perception, the frictional and normal forces are adjusted optimally in a way that depends on the topography of the surface (Adams et al., 2013). Moreover, several studies (Gerhardt et al., 2008; Gwosdow et al., 1986) shown the influence of perspiration and found that the resulting increase in skin friction enhanced the perception of roughness.

To conclude, simultaneous measurements of vibration and friction would establish whether tribological interactions play a significant role in modifying the vibratory response, which is currently regarded as the primary sensory cue in assessing fine surface texture. But, the fingerprint ridges and the large number density of sweat pores that are located in the ridges are the main physiological characteristics that explain the tribological complexity of a finger pad.

3- Muscle receptors

Receptors in and around skeletal muscles include stretch receptors, pressure pain endings with myelinated or unmyelinated afferent fibers, and paciniform corpuscles, which are located in facial planes and near interosseus ligaments. Paciniform corpuscles respond like Pacinian corpuscles in subcutaneous tissue. There are three types of stretch receptors (mechanoreceptor) in muscle, namely primary and secondary spindle receptors and the Golgi tendon organ. They provide the CNS with information about muscle length and force.

3.1 Primary and secondary spindle receptors

As suggested by their name, the primary and secondary spindle receptors are located within muscle spindles. Muscle spindles are elongated structures (see fig. 4) ranging in length from 4 to 10 mm. They are composed by bundles (up to 14) of small intrafusal fibers (M Swash, 1972).

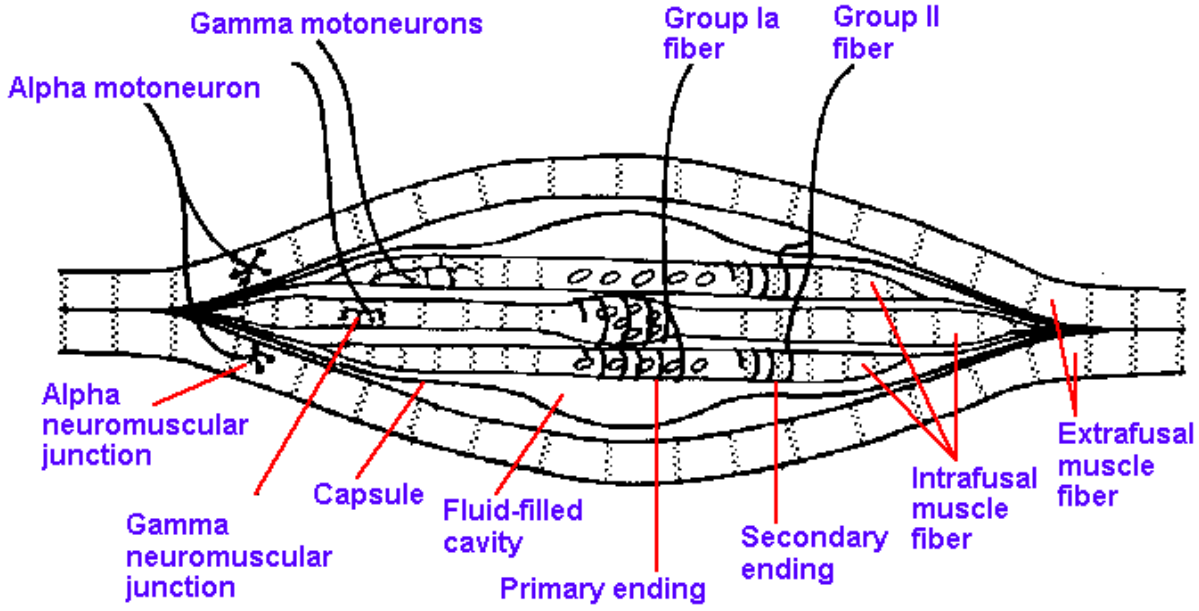

Figure 4: Sketch of a typical muscle spindle

The spindles lie parallel to the extrafusal muscle fibers, the force-generating components of muscle. They are scattered widely throughout the muscle body. There are two types of intrafusal muscle fibers: nuclear bag fibers and nuclear chain fibers. Nuclear bag fibers are thicker and longer than nuclear chain fibers, and they received

their name based on the accumulation of their nuclei in the expanded bag-like equatorial region known as the nuclear bag. Nuclear chain fibers have no equatorial bulge. The sensory innervation of the muscle spindle arises from both group A α (Ia) and group A δ (II) afferent fibers. The A α (Ia) fibers establish fiber coils around the equatorial regions of both the nuclear bag and the nuclear chain fibers, forming the primary muscle spindle receptors. Meanwhile, smaller A δ (II) fibers, which form the secondary muscle spindle receptors, terminate at either end of the nuclear region, primarily only on nuclear chain fibers. Intrafusal fibers are innervated by fusimotor neurons or gamma-motoneurons. Activity in fusimotor neurons produces a contraction of the bag and chain fibers, resulting in a stretch in the receptor-expressing equatorial region. The stretching of this central region, regardless of how it is accomplished, is adequate to stimulate primary and secondary spindle receptors. The fusimotor neurons or gamma-motoneurons should not be confused with the larger skeletomotor neurons or alpha-motoneurons, whose activity triggers the contraction of extrafusal fibers that produces muscle contraction.

Voss (Voss, 1971) estimated that there are 25,000–30,000 muscles spindles in the human body, including ~4000 in each arm. Within the hand, muscle spindle numbers range from just 12 in the abductor digiti minimi to 356 in the flexor digitorum superficialis. Higher spindle densities do not appear to be associated with superior sensory acuity as has been observed with the tactile sensory system.

Primary and secondary spindle receptors are both specifically responsive to changes in muscle length, but the former are much more sensitive to the velocity of contraction. Secondary afferents have much less dynamic responsiveness than primary afferents, and have a more regular discharge rate. This physiological distinction is consistent with the notion that primary spindle receptors signal the velocity and direction of muscle stretch or limb movement, whereas secondary spindle receptors provide information about static muscle length or limb position.

3.2 Golgi tendon organ

Golgi tendon organs are found near the muscle-tendon junction and buried deep within the tendon itself. The receptor consists of a specialized Aα (Ib) afferent terminal, with a delicate capsule that surrounds the nerve which, in turn, surrounds several fascicles of

tendon. The nerve fibers lie between fascicles in such a way that they can be "pinched" between them as muscles contract, and apparently thereby activated. In primate muscles, Golgi tendon organs are less numerous and more variable in number than spindle receptors (Devanandan et al., 1983). Some muscles, such as the lumbrical muscles, do not appear to have any tendon organs. As far as I know, there are no data for human tendon organs available. Of note, tendon organs are relatively insensitive to passive tension applied to the muscle by stretching it, but they are extremely sensitive to the active tension produced when the muscle contracts (Mann, 1981).

4- Up to the brain

Sensory information from receptors in the hand and from muscles controlling finger movements is conveyed via afferent nerve fibers to dorsal root ganglion neurons, which lie in the dorsal roots of the spinal nerves. The cell bodies of these neurons have two branches, one of which projects to the periphery and the other of which projects to the CNS. Smaller-diameter (Aδ and C) afferents mediating nociception and temperature diverge from the large-diameter (Aα) axons mediating touch and proprioception in the spinal cord. The two-axon groups project to the brain via different pathways, namely the anterolateral system (a.k.a. spinothalamic tract) and the dorsal column medial lemniscal (a.k.a. posterior column-medial lemniscus) pathway, respectively. Both pathways culminate in the thalamus, which then transmits signals to the neocortex (fig. 5). The axons of both pathways are segregated and arranged somatotopically as they ascend the spinal cord.

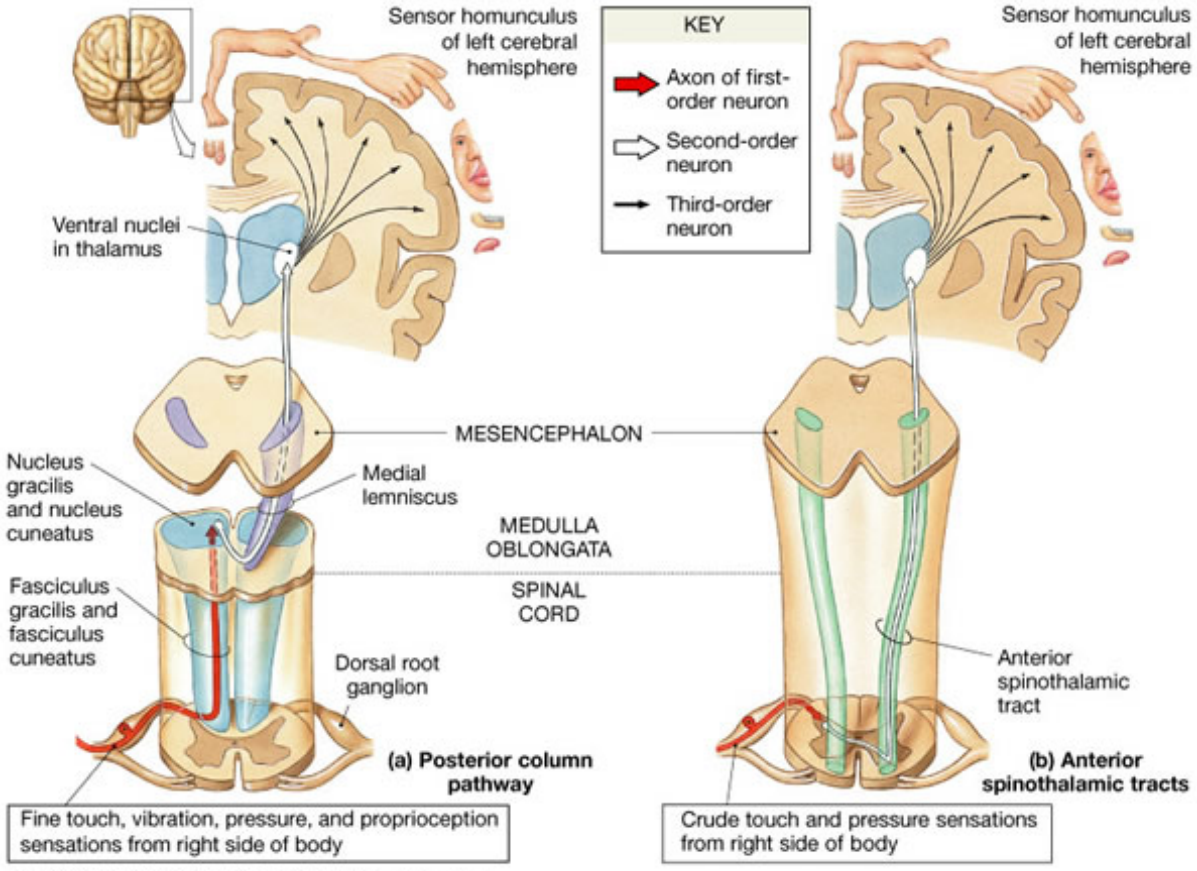

Figure 5: Both sensory pathways conveying sensory information from skin receptors up to the brain

4.1 Anterolateral system pathway

The anterolateral system consists of anterior and lateral constituents often called the anterior and lateral spinothalamic tracts (fig. 5). It carries information about pain, temperature, and light (poorly localized) touch (Olausson et al., 2002). Thinly myelinated (Aδ) and unmyelinated (C) nerve fibers (first order nerve fibers or protoneurons) convey nociception, temperature and light touch signals from the periphery. The relatively small neuronal cell bodies of these sensory axons are located in the dorsal root ganglia. Their central processes enter the spinal cord in the lateral part of the dorsal root, where they form collateral branches that ascend and descend several spinal segments in a region near the cap of the dorsal horn. These collateral branches enter the dorsal horn and synapse in the most superficial layers of the dorsal horn, in the segments above and below where they entered the spinal cord. Nociception, temperature, and light touch nerve fibers synapse on several cell types in the dorsal horn. Some of the recipient cells are local circuit neurons, including interneurons involved in motor reflexes. They also synapse on neurons involved in sensory transmission.

There are two groups of transmission neurons in the dorsal horn: (1) marginal (a.k.a. nociceptive-specific) neurons located in the most dorsal part of the dorsal horn, which respond almost exclusively to noxious inputs and appear to be most involved in signaling the presence and location of painful stimuli; and (2) wide dynamic-range neurons located deeper within the dorsal horn, which respond with increasing discharge frequency to more intense stimuli. The axons of these second-order transmission neurons comprise the anteriolateral (spinothalamic tract) system. Most of these axons decussate in the anterior white commissure of the spinal cord within a few segments of their origin; the remaining approximately 10% of axons that do not decussate ascend ipsilaterally. The decussating axons enter the anterolateral portion of the white matter of the spinal cord, where they ascend as the spinothalamic tract. The spinothalamic tract terminates mainly in the ventral posterolateral nucleus of the thalamus.

The somata of the third order neurons in the transmission of nociceptive, temperature, and light touch to the cerebral cortex are located in the ventral posterolateral nucleus (VPL) of the thalamus. VPL neuronal axons form topographic projections to the primary

somatosensory cortex S1 (Brodman's areas 3, 1, and 2 in the postcentral gyrus) via thalamic radiations.

4.2 Dorsal column medial lemniscal pathway

The dorsal column medial lemniscal pathway carries discriminative touch and proprioceptive information from the body to the brain. Importantly, the afferents carrying discriminative touch information are kept separate from those carrying proprioceptive information all the way up to the level of the cerebral cortex. The peripheral axons of the 1° afferents are myelinated, large or medium diameter axons. Each axon extends from a posterior root via a spinal nerve to its target in the periphery (i.e. skin, muscle, or joint), where it forms or innervates a somatosensory receptor. The 1° medial lemniscal afferents include A α axons that branch and terminate in the skin (innervating Merkel's cells or forming Meissner, Pacinian, or Ruffini corpuscles) as well as A α axons that terminate in the joints, Ia and II axons that branch in muscle spindles, and Ib axons that terminate in Golgi tendon organs within muscles.

The 1° medial lemniscal afferent central axons join a posterior root, enter the spinal cord, and ascend to the brain stem in the posterior column of the spinal cord (i.e. the medial lemniscal system). Approximately half of these medial lemniscal projections, known as propriospinal fibers, terminate at spinal levels. The remaining projections ascend in the posterior column of the spinal cord to the medulla without synapsing or decussating. The projections from the lower limbs and trunk form the gracile fascicle of the dorsal columns, and those from the upper arms form the cuneate fascicle of the dorsal columns. The gracile fascicle ascends medially while the cuneate fascicle ascends laterally. Thereafter, axons of the cuneate nuclei (2° afferents) pass anteriorly and decussate to form the medial lemniscus, contralateral to their cells of origin. Hence, above the level of the cuneate nuclei, each half of the body is represented contralaterally (i.e. left half of the body in right side of the CNS and *vice versa*) within the medial lemniscal pathway.

The 2° medial lemniscal afferents ascend in the medial lemniscus through the brain stem to the diencephalon. They terminate in the VPL nucleus of the thalamus. At the level of

the VPL, axons carrying cutaneous information terminate in the core of the VPL whereas those carrying proprioceptive information terminate in the surrounding shell of the VPL.

The 3° afferents of the dorsal column medial lemniscal pathway are thalamo-cortico neurons of the VPL, which travel in the posterior limb of the internal capsule and terminate in the cerebral cortex. The VPL projects to Brodmann's areas IIIa, IIIb, I, and II in the primary somatosenry cortex S1 located in the post-central gyrus of the parieatal lobe.

In 1909, Brodmann published his cortex mapping based on cell types or cytoarchitecture and distributions. He divided the human brain in 47 areas in each hemisphere. Remarkably, the Brodmann divisions, which were based on early 10^{th} century technology such as light microscopy, still have functional significance today. The cerebral cortex has a well-recognized outer surface characterized by fissures (or sulci) and folds (or gyri). It is divided into four major lobes: frontal, parietal, occipital and temporal. The central sulcus (Rolando) dividing the frontal and parietal lobes is the key landmark for locating S1 (which includes Brodmann's areas 3, 1, and 2). S1 is an area of granular cortex identifiable anatomically as the postcentral gyrus situated directly behind the central sulcus in the parietal lobe,

S1 can be subdivided into four subregions based on afferent inputs: IIIa (muscle afferents), IIIb and I (fast and slowly adapting cutaneous afferents, respectively), and II (joint afferents). Most of the thalamic inputs terminate in subregions IIIa and b, and the cells in these subregions project to subregions I and II. There are some direct thalamocortical projections to subregions II and I, but they are relatively few in number. Mima et al. (Mima et al., 1997) showed that the subregions of S1 differ in terms of the inputs they receive from the thalamus. Specifically, signals from skin receptors are received in subregions IIIb and I, whereas proprioceptive information is transmitted to subregions IIIa and II. Subregion II of S1 has a considerable amount of projections to the motor cortex. Each of the four subregions of S1 contains a full representation of the body. As emphasized by Buonomano et al. (Buonomano and Merzenich, 1998), these cortical maps of the body are dynamic and modified as a function of one's personal experience.

5- Roughness perception

Information about the external world is acquired and subdivided into separate processing streams in each of the sensory systems (as discussed above). This division begins at the very first stage of processing: at the level of nociceptors, thermoreceptors, proprioceptors, and mechanoreceptors, which transduce different stimulus properties and channel their information into separate, parallel streams. Evidence from psychophysical and neurophysiological research indicates that what is perceived as tactile perception is a conglomerate of all of these functionally distinct streams of information.

Animals, including humans, can engage in active or passive forms of touch. Active touch refers to the act of purposeful touching, and implies voluntary, self-generated movements intended to gather information about the properties of surfaces (texture, hardness, temperature) and/or objects (size, shape, weight, location). Passive touch, on the other hand, refers to the state of being touched and implies that an external agent is generating the sensory input. For both modes of touch, the sensory input can be either *static* (no movement) or *dynamic* (movement between the skin and the object). According Lederman et al.'s (Lederman and Klatzky, 1987) definition of an exploratory procedure —i.e., a stereotyped movement pattern having certain characteristics that are invariant and others that are highly typical in the function of working toward the goal of a task—hand movements made during an exploration task can be classified reliably as exploratory procedures.

The research of the present theses is focused on a singular component of the expansive realm of tactile perception, namely roughness perception. People engage in spontaneous rubbing of surfaces as a means of exploring texture when they are asked to make textural judgments. Regardless of the size or location of skin used, or the mode of touch engaged in, this form of exploration always involves relative (e.g. lateral) motion between the skin and the textured surface being explored.

Although the term roughness is ubiquitous, its precise meaning is ambiguous. Smith et al. (Smith et al., 2002) suggested an interesting definition:

> *Roughness is the mental product of an integrative perceptual process, whereas texture refers to the topographical irregularities measured in units of*

horizontal and vertical distance between the peaks and valleys (or ridges and groove width)

The complexity of the roughness perception experience suggests that there is more than one physiological mechanism or code of tactile information used in the perception of roughness. Currently, it is collectively admitted that at least two codes exist for roughness (Hollins and Risner, 2000): a spatial code that accounts for coarse and medium properties; and
a vibrotactile code that carries information about very fine surfaces (e.g. the spatial period or center-to-center distance between texture elements that are <200 μm). These codes depend on signals that are generated in different classes of mechanoreceptors and are processed by distinct cortical algorithms.

The first prominent model of texture perception, namely the duplex theory of tactile texture perception, was introduced by Katz in 1935 (Katz, 2013). That theory, however, was overshadowed in subsequent decades. Compelling evidence indicating that roughness is closely associated with spatial properties emerged (Lederman and Taylor, 1972; Taylor and Lederman, 1975). However, the perception of roughness seemed to be largely independent of scanning velocity in these studies, which used stimuli with a relatively high spatial period (> 500 μm). Tactile roughness perception is commonly studied using periodic surfaces, such as gratings of alternating ridges and grooves, or dot patterns. The spatial period of a grated stimulus is defined as the sum of the cross-sectional groove width (i.e. inter-element spacing) and ridge width (i.e. element width). Interestingly, Cascio et al. (Cascio and Sathian, 2001) found that groove width has a greater effect on perceived roughness than does ridge width, confirming earlier studies (Taylor and Lederman, 1975), (Sathian et al., 1989). On the other hand, the work of Cascio et al. (Cascio and Sathian, 2001) contradicted previous studies suggesting that temporal factors do not contribute to estimates of roughness magnitude. When Hollins and Risner (Hollins and Risner, 2000) measured the discriminability of pairs of fine surfaces (mean spatial periods of 18 μm and 30 μm), they observed chance-level performance in the absence of movement, but nearly perfect performance when movement was incorporated. Their work further suggested that the transition from fine to coarse processing mechanisms occurs at a spatial period of around 200 μm. Subsequently, they advanced the view that roughness perception is mediated by systems that are highly sensitive to vibration (Hollins Sliman J Bensmaïa Sean W, 2001).

A central question in the area of roughness perception is what is the physiological basis of roughness, and related to this question, what are the physiological mechanisms of spatial coding and vibratory coding in particular. To address this question, human psychophysical data were compared with Macaque neurophysiological data in a series of studies (Blake et al., 1997a; 1997b; Connor et al., 1990; Yoshioka et al., 2001). The approach of these studies consisted of associating the activity patterns in populations of peripheral afferent fibers in the Macaque that were evoked by various textured surfaces to estimates of the perceived roughness of the same textures from human psychophysical experiments. Ultimately, there was only one neural code that emerged as a viable basis for roughness perception: spatial variation in SA1 firing rates. Briefly, for widely spaced surface elements, the spatial variation in firing rates was found to be determined primarily by the surface pattern. Meanwhile, for finely spaced elements, the variation in firing rates between SA1 afferents was found to be related to stochastic variation in spike rates. However, it appears that roughness of fine surfaces is not spatially coded. We can use of our ability to detect the fine vibrations generated by the movement created by the exploratory procedure to obtain spatial information.

Hollins and colleagues conducted a series of experiments examining the role of SA1 mechanoreceptors in the coding of vibration (Bensmaïa and Hollins, 2005), (Bensmaïa and Hollins, 2003), (Hollins et al., 2002). Based on their work, they concluded that the vibrotactile code underlying perceived roughness of finely textured surface is determined by the intensity of vibrations produced in the skin during scanning. They also suggest that the peripheral neural code for perceived roughness is essentially the total activity evoked in the Pacinian system.

The dual nature of fine versus coarse roughness perception suggests that each code (fine or coarse) operates most effectively over a range of texture scales where the other code is weak. The most compelling evidence suggesting that both codes can contribute to roughness perception comes from a study by Gescheider et al. (Gescheider et al., 2005). It was demonstrated in these experiments that subjects were not only able to switch their attention between vibratory and spatial codes, but also able to combine these two types of signals into a unified percept.

The question of what happens at the level of the brain during roughness perception is beginning to be answered. Neuroimaging techniques like fMRI (functional magnetic

resonance imaging) may aid in the identification of regions of the human brain that are involved in tactile roughness perception. Trulsson et al. (Trulsson et al., 2001) combined fMRI with microneurography to obtain more detailed information about the representation of the body surface in sensory cortex. They observed a surprisingly large hemodynamic response to microstimulation in S1. Moreover, lesions within S1 (IIIa, IIIb, II, or I) result in perceptual impairments in tasks that require processing of the affected modality. In monkeys (Randolph and Semmes, 1974), areas IIIa and IIIb have been shown to be important for different kinds discrimination tasks, with lesions of the former resulting in severe impairments in the performance of hard-soft, roughness, and shape discrimination tasks, and lesions of the latter affecting tactile discrimination task performance.

In conclusion, roughness perception can be predicted from the combined responses of Merkel cell/SA1, Pacinian corpuscle/RA2, and (to a lesser extent) Meissner corpuscle/RA1 systems, with signals from these three populations of afferents remaining segregated until the early stages of cortical processing. The involvement of three afferent types in roughness perception is discordant with the previously accepted idea that SA1 signals are solely responsible for conveying texture information.

6- Purpose of the thesis

The main question underlying the pursuit of this is: what would motivate a hand surgeon to study the roughness perception of the fingerpad? As hand surgeons, we tend to focus on mechanical aspects of the hand. But the human hand is much more than bones and joints animated by nerves and tendons. Moreover, the ability to feel is critical for manual dexterity. Tactile information tells a person how much force to use when grasping objects, which range from rigid, such as a steel marble. to delicate, such as a tomato. Researchers are currently working on developing prosthetic systems that incorporate touch-sensitive feedback. Understanding the neurobiology of roughness perception could be revolutionary to the utility of hand prosthetics.

As reviewed in the Introduction, roughness perception requires the combination of at least two codes, a spatial code mediated by Merkel cell/SA1 afferents and a vibrotactile code mediated by the Pacinian corpuscle/RA2 afferents. However, it remains unclear how these systems cooperate in roughness perception. Moreover, most studies of roughness perception are carried out with stimuli formed by a highly-structured raised dot pattern. However, diverse and irregular textures are often perceived in daily life.

The first step of the present work was to choose a set of "realistic" stimuli and an exploratory procedure that approximates natural exploration of texture inasmuch as it is possible. We elected to use a complete set of sandpapers varying in average particle size from 18 µm to 195 µm as our stimulus set. For the exploratory procedure, we chose an active dynamic touch strategy in which subjects were blindfolded without auditory cues.

The second step consisted of developing and validating a psychophysical method to estimate roughness threshold with the sandpaper set. A double interlaced adaptive staircase procedure based on a two-alternative forced choice paradigm was adopted for this validation testing.

In chapter 2, I report an investigation of the relationship between the roughness discrimination threshold and the tactile spatial resolution threshold at the fingerpad level, and how it changes across the human lifespan.

In chapter 3, I examine the relative contribution of remote mechanoreceptors to perception of roughness versus spatial acuity in various conditions that affect innervation of the index finger differently. Compared conditions include unilateral carpal tunnel syndrome, surgically repaired complete traumatic median nerve section at the wrist; and a control condition consisting of ring-block anesthesia of the entire index finger as a model of pathological denervation of the fingertip.

Finally, in chapter 4, I summarize the contributions of this thesis to the field of roughness perception, provide new global hypotheses regarding the mechanisms involved, describe possible future investigations, and discuss some relevant practical ramifications of the findings.

Chapter 2: Tactile roughness discrimination threshold is unrelated to tactile spatial acuity.

Libouton X, Barbier O, Plaghki L, Thonnard JL.
Tactile roughness discrimination threshold is unrelated to tactile spatial acuity. Behav Brain Res. 2010 Apr 2; 208(2):473-8.

2.1- Abstract

The present study examined the relationship between the tactile roughness discrimination threshold (TRDT) and the tactile spatial resolution threshold (TSRT) at the index fingertip in humans. A new device was built for measuring TRDT, allowing pair-wise presentations of two sets of six different sandpaper grits. The smoothest grits ranged from 18 to 40 µm and the roughest grits ranged from 50 to 195 µm particle size. The reference sandpaper had a 46 µm particle size. A two-alternative forced choice paradigm and a double interlaced adaptive staircase procedure yielding a 75% just noticeable difference (75%jnd) was used according to Zwislocki and Relkin (Zwislocki, 2001). Contact force and scanning velocity were measured at the fingertip with a built-in sensor. The TSRT was assessed with an extended set of grating domes. Fifty-three male and female subjects, spanning a wide age range participated in this study. The JND75% or TRDT was lower for the smoothest sandpapers (15 ± 8.5 µm) compared to the roughest sandpapers (44 ±32.5 µm). TRDT performance was unrelated to age or gender. Additionally, grit size had no effect on the mean forces (normal and tangential) exerted at the fingertip or the mean scan velocities. In contrast, there was a significant degradation of TSRT performance with age. Lastly, there was no significant correlation between TRDT and TRST performance.
Results of this study support the theory that the neural mechanisms underlying the perception of tactile roughness discrimination for fine textures differ from those involved in spatial resolution acuity often associated with the SA1 afferents.

2.2- Introduction

Early in the twentieth century, David Katz (Katz and Krueger, 1989) argued that coarse texture perception is primarily mediated by spatial encoding while fine texture perception is primarily mediated by temporal encoding (e.g., vibrotaction). This conception has been called the "duplex theory of tactile texture perception" (Hollins, 2010; Johnson and Hsiao, 1992). Subsequently, the validity of this theory was questioned on empirical grounds. For instance, Lederman & Taylor(Lederman and Taylor, 1972), using a series of precisely machined metal gratings as stimuli, found that the spatial parameters of gratings exerted a chief influence on texture perception, while the speed of movement of the fingertip across the grating contributed little to texture discrimination. Connor and Johnson (Connor and Johnson, 1992) further compared the relative ability of hypothetical spatial and temporal coding mechanisms to account for roughness perception. They examined the neural basis of spatial encoding in monkeys and their findings implicated the involvement of slow adapting type 1 (SA1) mechanosensitive afferents, rather than those mediating vibrotaction. In recent years, however, new experimental evidence has accumulated to support Katz's view that vibrotaction plays a role in the perception of textures whose elements are too small and closely spaced to be processed spatially (Hollins et al., 2002) and even for the perception of relatively coarse textures(Cascio and Sathian, 2001; Gamzu and Ahissar, 2001). Currently, it is assumed that spatial and temporal coding mechanisms can operate in isolation, but that in ecological conditions they work together to enhance the tactile perception of texture.

Texture perception is multidimensional with two orthogonal dimensions: roughness/smoothness and hardness/softness(Hollins et al., 1993). Most research examining tactile texture perception has focused specifically on the highly prominent perceptual dimension of roughness. The present experiments dealt chiefly with this perception. More precisely, we aimed to determine the just noticeable difference (JND) threshold for roughness discrimination under moving conditions(Gescheider, 1997). For this purpose, we designed and built a device that allows pair-wise presentations of sandpapers with different particle sizes in a two-alternative forced choice procedure. Furthermore, to characterize the moving conditions, the sandpapers were mounted on a

3D force plate allowing measurement of the force exerted by the fingertip and the scanning velocity of the lateral movement. We hypothesized that force and scanning velocity may be related to texture discrimination performance, as subjects may spontaneously alter these variables for optimal performance. Finally, to further explore the involvement of spatial and temporal coding mechanisms in the perception of roughness, we also measured tactile spatial threshold, using the well-known grating orientation task (Craig and Johnson, 2000; Gibson and Craig, 2002; Tremblay et al., 2003; Van Boven and Johnson, 1994a).

2.3- Materials and Methods

2.3.1- Subjects

Fifty-three healthy subjects (28 women and 25 men) participated in the study and were recruited among students of the Université catholique de Louvain and members of their families. All subjects underwent a diagnostic interview by a physician and were included in the study when considered free from diseases or injury that could affect the tactile sensitivity of their hands. Subjects were between 7 and 90 years of age. No inducement was offered for participation. The Ethics Committee of the Université catholique de Louvain approved the experimental procedures, and all subjects, including the parents of child subjects, gave written informed consent.

2.3.2- Test descriptions

2.3.2.1- Roughness discrimination task

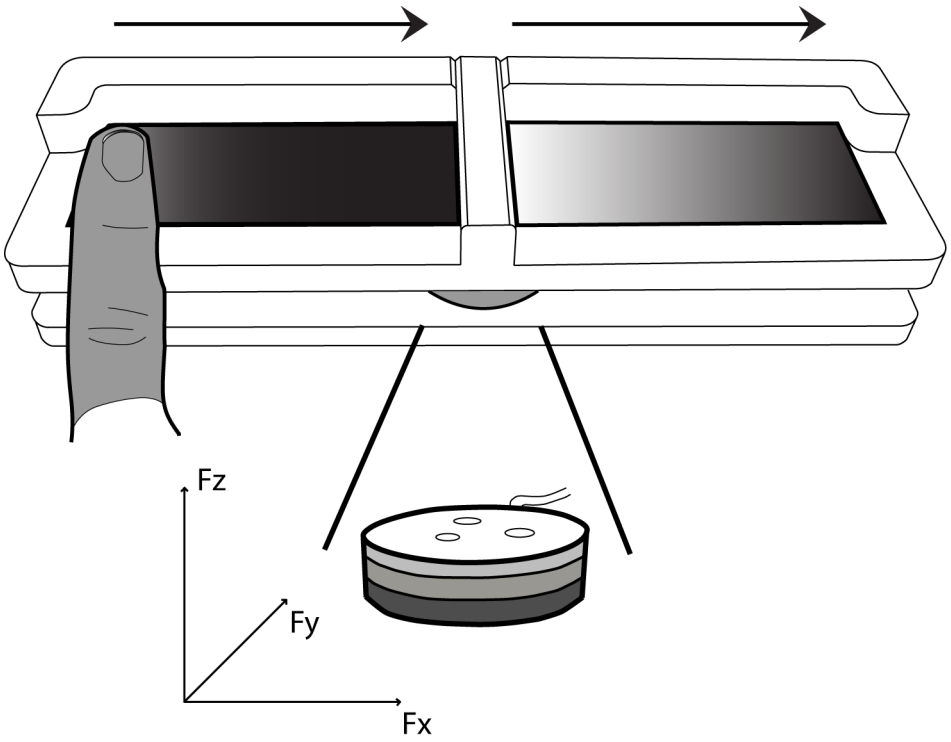

Figure 6: Device designed for roughness discrimination threshold measurement

The subject was comfortably seated at a table facing the experimenter and was requested to position the index of the dominant hand just in front of two textured surfaces, each 7.5 x 3.0 cm (fig. 6).

A cardboard screen was placed over the participant's wrist to block the view of their hand. Without further instructions, the participant was asked to slide the fingertip of their index finger on the first stimulus (located on the left side) and then subsequently on the second stimulus (located on the right side). After each trial, the participant was asked to discriminate the textures by reporting which was the rougher surface. Between trials, the subject raised their index finger to allow the experimenter to reposition it on the left side for the presentation of the next stimulus. The subject scanned each stimulus with a single sweep using contact force and scanning velocity that seemed to be most appropriate to them. Headphones were used to muffle any extraneous noise.

Thirteen sandpapers (see table 1), with average grit sizes varying from 18 μm (grit number P1000 – the smoothest stimulus) to 195 μm (grit number P80 – the

roughest stimulus) were used as stimuli. The set of sandpapers used for this study came from the same manufacturer (SIA abrasives industries®). Grit number and particle size ("micron grade") were according to the Federation of European Producers of Abrasive Products (FEPA) P-grading system.

Table 1: Set of sandpapers

	Stimulus N°	FEPA* P-grade	Average grit size (µm)
Smooth	13	P1000	18
	12	P800	22
	11	P600	25.8
	10	P500	30
	9	P400	35
	8	P360	40
Reference Surface	7	P320	46
	6	P240	58
	5	P220	65
	4	P180	78
	3	P120	127
	2	P100	156
Rough	1	P80	195

*Federation of European Producers of Abrasives

Two tactile roughness discrimination thresholds (TRDT) were determined using a double interlaced adaptive staircase procedure based on a two-alternative forced choice paradigm (figure 5). The stimulus dimension at which static information does not contribute significantly to texture discrimination has been estimated to be ≤ 100 µm (Hollins and Risner, 2000). Therefore we choose P320 sandpaper (average particle size

of 46 μm) as our reference stimulus (i.e. about halfway between 100 μm and full smoothness). The reference was present in each trial and randomly located on the left or right side. The first and second staircase started with the P800 (smooth) and P100 (rough) stimuli, respectively. After each trial, we moved from one staircase (smooth or rough) to the other (see fig. 7). As a result, odd trials were comprised of the staircase in which the smoother textured stimuli (P800 to P360) were compared to the reference (P320) while even trials were comprised of the staircase in which the rougher textured stimuli (P100 to P240) were compared to the reference. We measured the tactile roughness discrimination threshold, which was defined as the amount of change required to produce a 75% just noticeable difference (75%jnd) in sensation. The stimulus difference was defined as the difference in particle size between a given stimulus and the reference stimulus (P320). Using the algorithm proposed by Zwislocki & Relkin(Zwislocki, 2001), the rules for stimulus difference (or intensity variation) were as follow: in each staircase, after every incorrect response, the stimulus difference was increased; after three correct responses, not necessarily in consecutive order, the stimulus difference was reduced (see fig. 7). The procedure was discontinued when in the same staircase (smooth or rough) the number of up and down stimulus differences after the first mistake was equal. In this way, in each staircase, the stimulus difference was expected to track the 75% correct response threshold, i.e. the 75% just noticeable difference (75%jnd). A few subjects were able to correctly discriminate the smallest difference in particle size (P240 and/or P360 against reference P320). Their discrimination performance exceeded the limit of resolution of the stimuli. For these subjects, we allowed a threshold value of half the smallest difference in particle size.

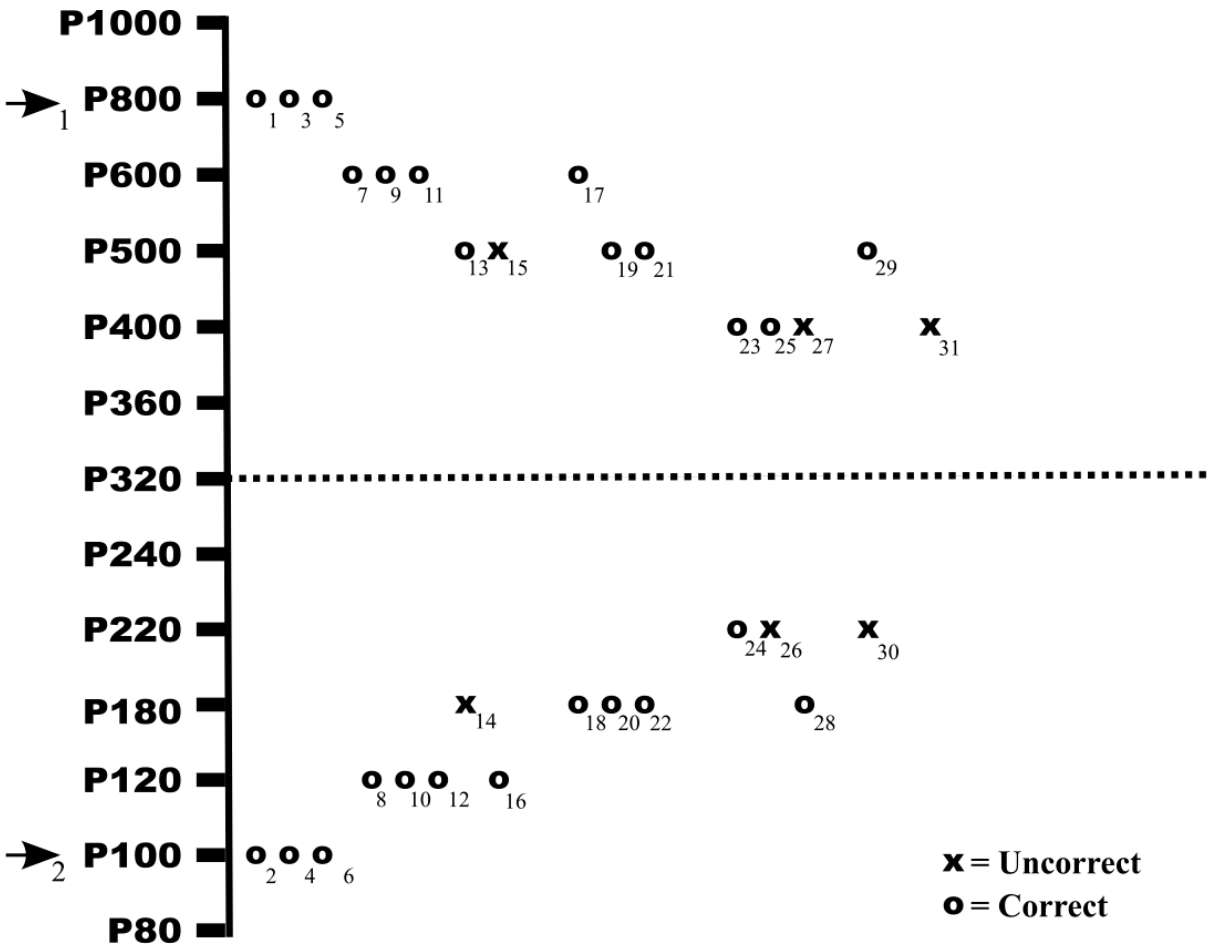

Figure 7: Double adaptive staircase procedure for both rough and smooth tactile discrimination thresholds. Arrows indicate the starting point of each staircase. The numbers below each response correspond to the order of presentation of each stimulus.

2.3.2.2- Apparatus

Sandpapers were mounted on a platform (fig. 6) linked to a force-torque sensor (Mini 40 F/T transducer; ATI Industrial Automation, NC, USA). The sensor measured the three force (Fx, Fy, Fz) components exerted by the fingertip on the platform. The sensing ranges for Fx, Fy and Fz were ± 40 N, ± 40 N and ± 120 N with 0.01 N, 0.01 N and 0.02 N nominal resolutions, respectively. The torques and forces measured by the sensors were used to determine the center of pressure (CP) at the index fingertip with the following equation:

$$CP = T/Fz$$

Where T, and Fz correspond to the torque and normal force, respectively. The CP

indicates the coordinates of the point at which the resultant Fz should be applied to generate the measured torque (T). The mean scan velocity was calculated on every trial from the CP displacement. The signals from the force transducers were digitized on-line at 200 Hz with a 12-bit 6071E analog-to-digital converter in a PXI chassis (National Instruments, Austin, TX, USA). After analog-to-digital conversion, the signals were further low-pass filtered with a fourth-order, zero phase-lag Butterworth filter having a cut-off frequency of 15 Hz. The following temporal variables were measured (see fig. 8): 1) the loading phase (T1-T2), defined as the delay between the onset and the peak of the tangential force and (2) the scanning phase (T2-T3). Also measured during the scanning phase were: 1) the mean tangential force; (2) the mean normal force; (3) the mean scanning velocity.

Figure 8: Example of normal force, tangential force and center of pressure (Cpdx) recorded during the scanning of a given surface

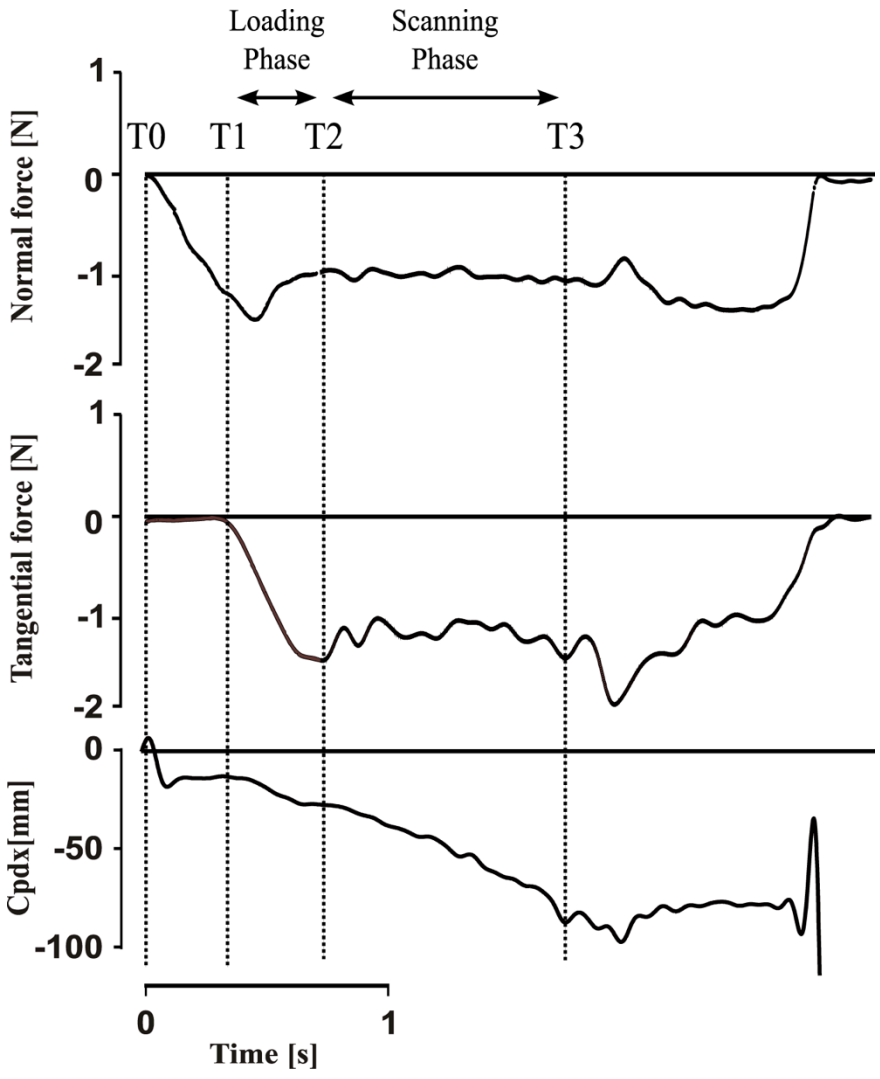

2.3.2.3- Tactile spatial resolution acuity

Tactile spatial resolution threshold (TSRT) was measured with the Grating Orientation Task (GOT) using JVP Domes (JVP Domes, Stoelting Co., Wood Dale, IL) on the index finger of the dominant hand. This test consists of a set of eleven different hemispherical plastic dome gratings having equidistant bar and groove widths: 0.35, 0.50, 0.75, 1.00, 1.20, 1.50, 2.00, 3.00, 3.50, 4.00 and 4.50 mm. Each dome was applied perpendicularly to the skin for 1-2 s with a skin indentation between 1-2 mm. The domes were randomly aligned in one of the two orthogonal directions (i.e. with the grooves parallel or transverse to the long axis of the index finger). Blindfolded subjects were required to identify the stimulus orientation before the stimulus was removed. A procedure adapted from that of Van Boven and Johnson (Van Boven and Johnson, 1994a) was used(Bleyenheuft et al., 2006). The 3 mm grating was first applied for ten consecutive trials using a randomized orientation of the bars. If the subject succeeded the next smaller grating (2 mm) was applied. If the subject failed, the next larger grating (3.5 mm) was applied. The test was stopped when the probability of correct answers for the grating reached approximately 50%. The tactile spatial resolution threshold was a simple linear interpolation estimate of the 75% correct grating width. A lower tactile acuity grating score (TAG score) signified better tactile spatial resolution acuity.

$$TAGscore = g_{below} + \frac{0.75 - p_{below}}{p_{above} - p_{below}}(g_{above} - g_{below})$$

Where g = grating width of a probe, p = probability of correct answers, *above* = the grating width that results in a score closest to but above 75% correct, and *below* = the grating width that results in a score closest to but below 75% correct.

2.3.3-Statistics:

Non-parametric statistics were used when normality tests failed or when statistics were performed on ordinal data. Hence a Mann-Whitney U test was used to analyze the effect of sex on the roughness discrimination threshold and a Wilcoxon paired rank test was performed for paired samples. A one-way analysis of variance (ANOVA) was performed on effect of age on the roughness discrimination threshold. For describing the relationship between two variables, Spearman's rank correlation coefficient was computed.

2.4- Results

Examples of the temporal variation of the normal and tangential forces, as well as the vertical component of the CP during a typical trial are represented in figure 8. T0 represents contact with the stimulus. Normal force was increased up to around 1N. During the loading phase (T1-T2) the tangential force was increased while the CP was slowly altered due to the skin's compliance. At the end of the loading phase, slipping occurred and the scanning phase (T2-T3) started. During this phase the CP changed continuously. The mean scan velocity was calculated as the first time derivative of the CP displacement.

2.4.1- Roughness discrimination thresholds

The two 75%jnd or TRDTs were measured for each subject: (1) the "smooth threshold", on average 14.7 ± 8.5 µm, expresses the ability to discriminate the smoothest stimuli (S1 to S6) against the reference stimulus and (2) the "rough threshold", on average 43.5 ± 32.5 µm, expresses the ability to discriminate the roughest stimuli (R1 to

R6) against the reference stimulus. Subjects showed a higher performance rate in difference threshold for the set of smooth sandpapers as compared to performance with the set of rough sandpapers (fig. 9).

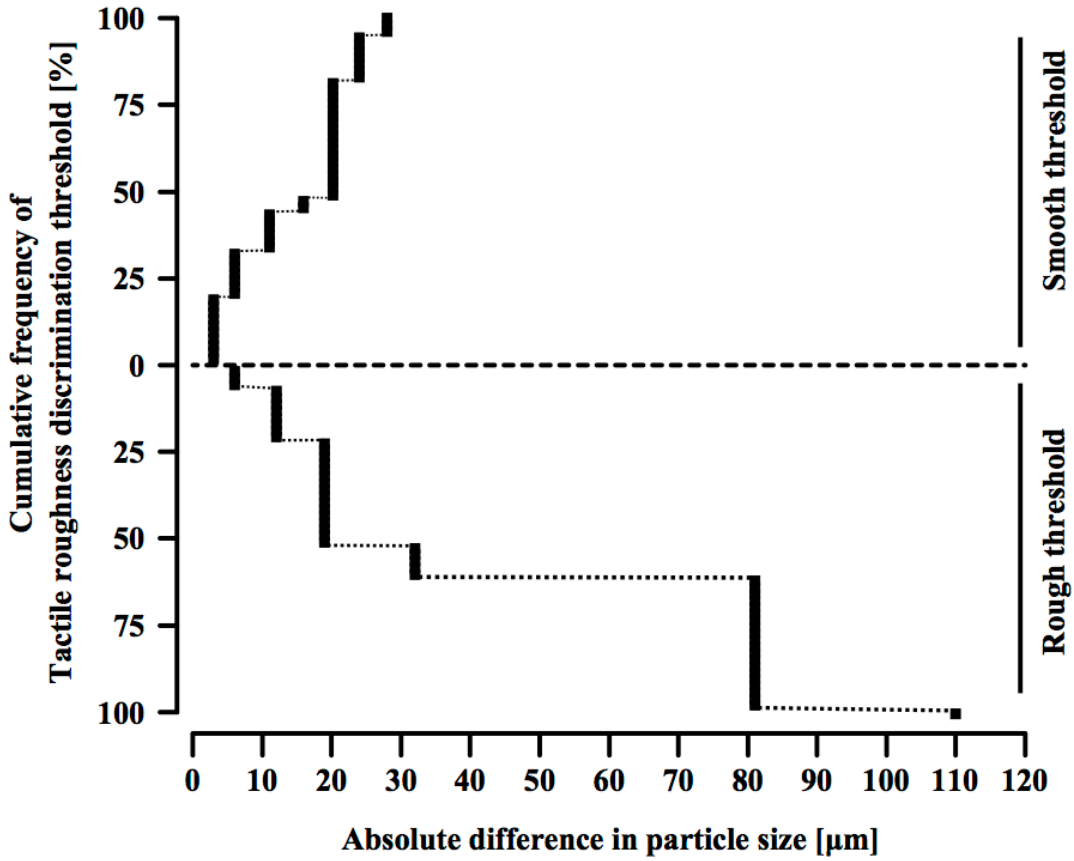

Figure 9: Cumulative frequency distribution of roughness discrimination thresholds for the set of smooth and the set of rough sandpapers as a function of the absolute difference in particle size between a given sandpaper and the reference sandpaper (particle size of 46 µm). Performance was higher for the set of smooth sandpapers as compared to the performance with the set of rough sandpapers.

There was a significant within-subjects correlation between both thresholds (Spearman's rho = 0.43; p = 0.001). There was no effect of age on TRDT for either the rough or smooth staircase (figure 10, Spearman's rho = 0.11, p = 0.35 for the rough threshold and rho = 0.13, p = 0.36 for the smooth threshold). Similarly, there was no effect of gender on TRDT (Mann-Whitney U test; p = 0.42 for the rough threshold and p = 0.13 for the smooth threshold, results not shown).

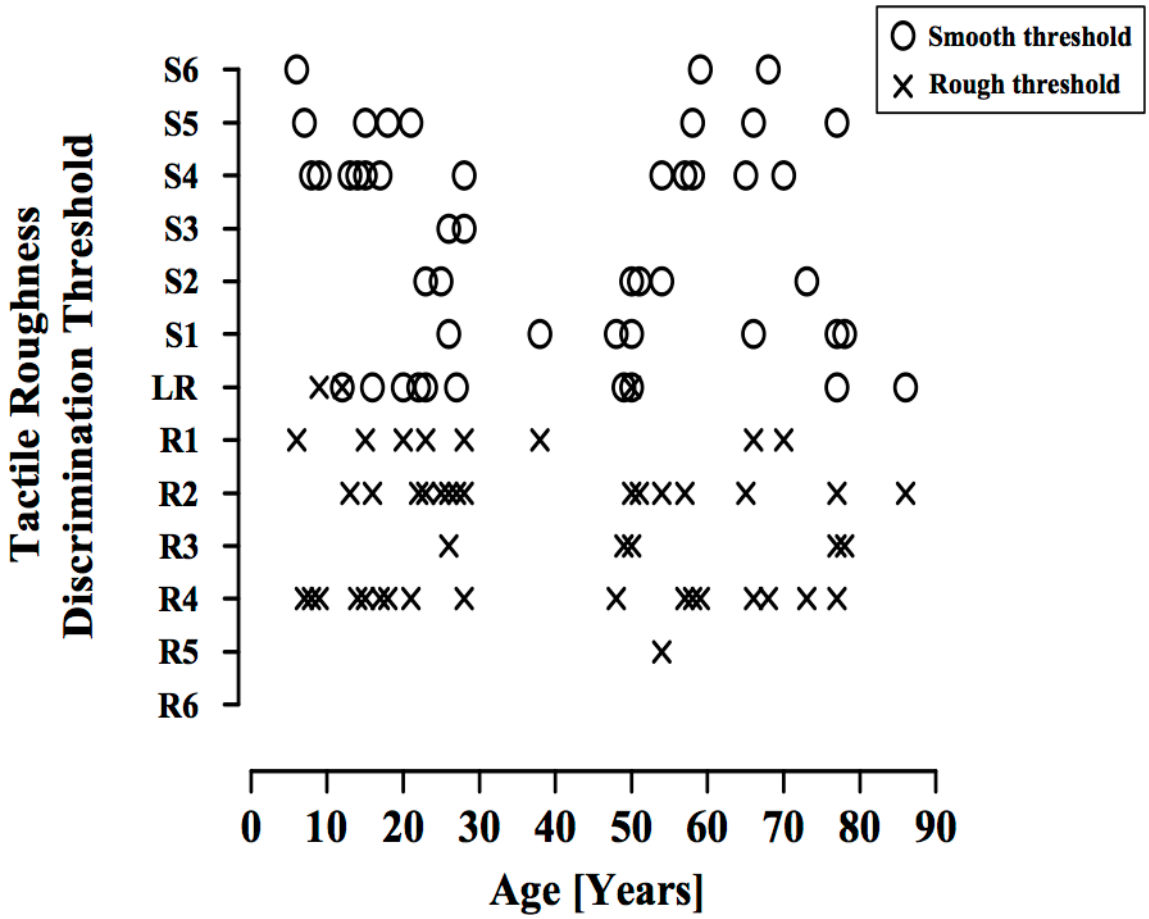

Figure 10: Effect of age on tactile roughness discrimination threshold for the smooth (S1 – S6) and rough (R1 – R6) set of sandpapers. LR represents the limit of resolution.

These results were reliably reproduced in eleven participants who were evaluated a second time three months after the first evaluation. There were no significant differences in measurements for the TRDT with the set of smoothest stimuli or with the set of the roughest stimuli (Wilcoxon's paired rank test, $p = 0.42$ and $p = 0.94$, respectively).

The frequency distributions of mean normal force, mean tangential force and mean scanning velocities for all subjects are shown in figure 11. The distributions of the normal and tangential forces are skewed to the right with a median value and interquartile range of 1.1 N [0.7 – 1.9] and 1.3 N [1.0 – 2.3] respectively. The scanning velocity was normally distributed with a mean value of 52 ± 40.3 mm/s.

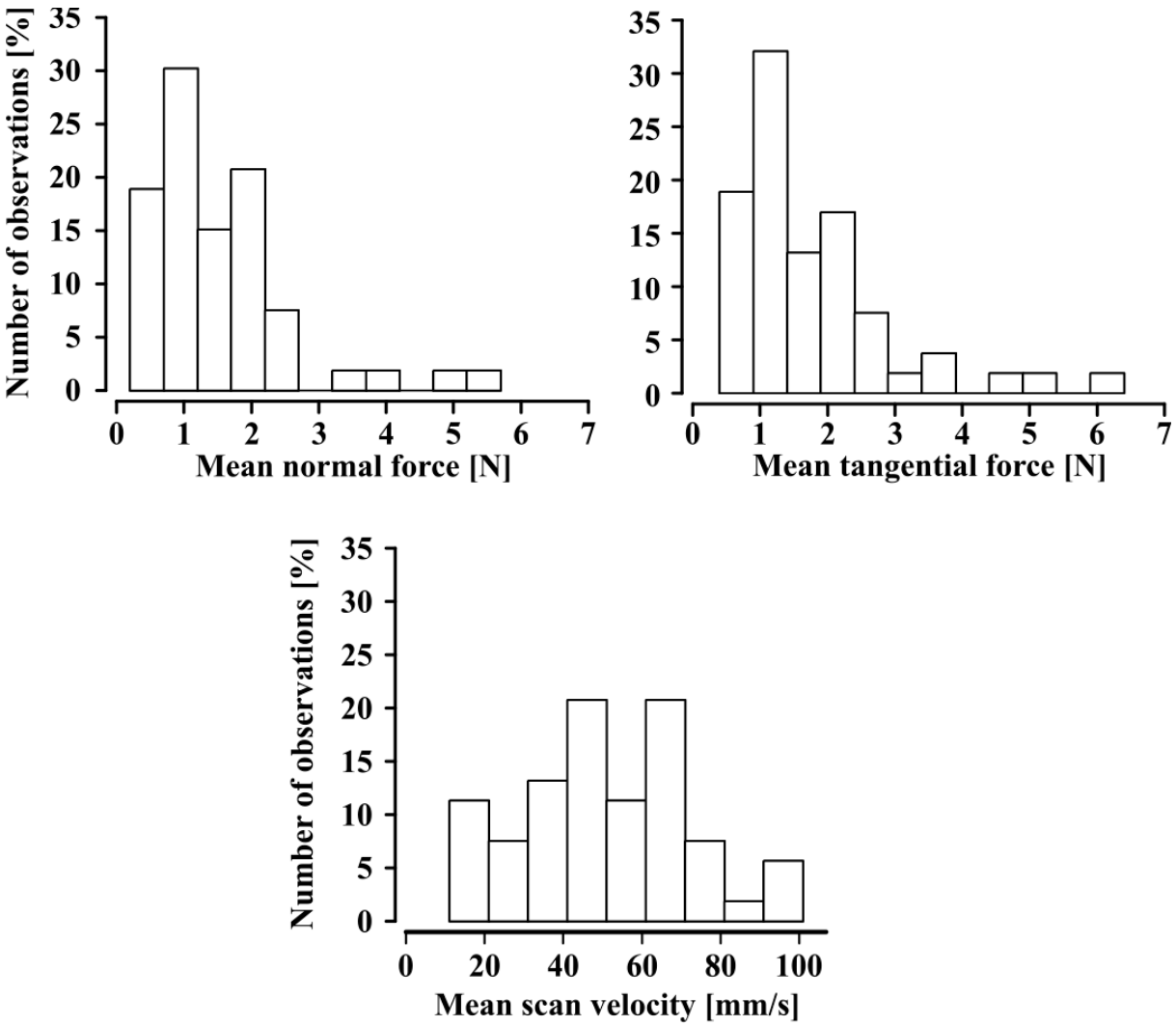

Figure 11: Relative frequency distributions of the mean normal force, the mean tangential force and the mean scanning velocity used by each subject when exploring the sandpaper surfaces. While normal force and tangential force distributions were skewed to the right, scanning velocity showed a normal distribution

There was no significant correlation between age and the normal force ($r = 0.266$; $p > 0.1$), the tangential force ($r = 0.258$; $p > 0.1$) and the mean scanning velocity ($r = 0.033$; $p > 0.1$). Finally, particle size had no effect on any of the measures acquired to characterize the lateral movement of the fingertip against the sandpapers. In addition, particle size did not affect the TRDT for the fine textures or for the coarse textures (Table 2).

	Mean scan velocity	Mean normal force	Mean tangential force
Threshold for smooth sandpaper	0.25 p = 0.07	0.17 p = 0.21	0.11 p = 0.43
Threshold for rough sandpaper	-0.09 p = 0.53	-0.13 p = 0.34	-0.26 p = 0.06

Table 2: Spearman's rank order correlation square (R^2) for mean scanning velocity and mean forces exerted at the fingertip in relation to the tactile roughness discrimination thresholds for the set of smooth and of rough sandpapers.

2.4.2- Tactile spatial resolution thresholds

The average tactile spatial resolution thresholds (TSRTs), measured with the Grating Orientation Task (GOT) with respect to age, are presented in table 2. There was a significant decrease in discrimination performance with age. Subjects above 65 years of age required a grating width about 3 times greater than those in the youngest age group (7-15 years) in order to perform at threshold ($t = 3.55$; $p < 0.001$).

There was no significant relationship between performance in the GOT and performance in the TRDT (figure 12; $r = 0.124$ with $p > 0.4$ for the staircase with the smooth textures and $r = 0.029$ with $p > 0.8$ for the staircase with the rough textures).

Age groups (years)	**N**	**Threshold (mm)**
7 - 15	12	1.3 ±0.8
16 - 39	15	1.8 ±0.7
40 - 64	15	2.5 ±0.8
65 - 90	11	3.5 ±0.5

Table 3: - Spatial resolution thresholds for different age groups (mean ±vsd)

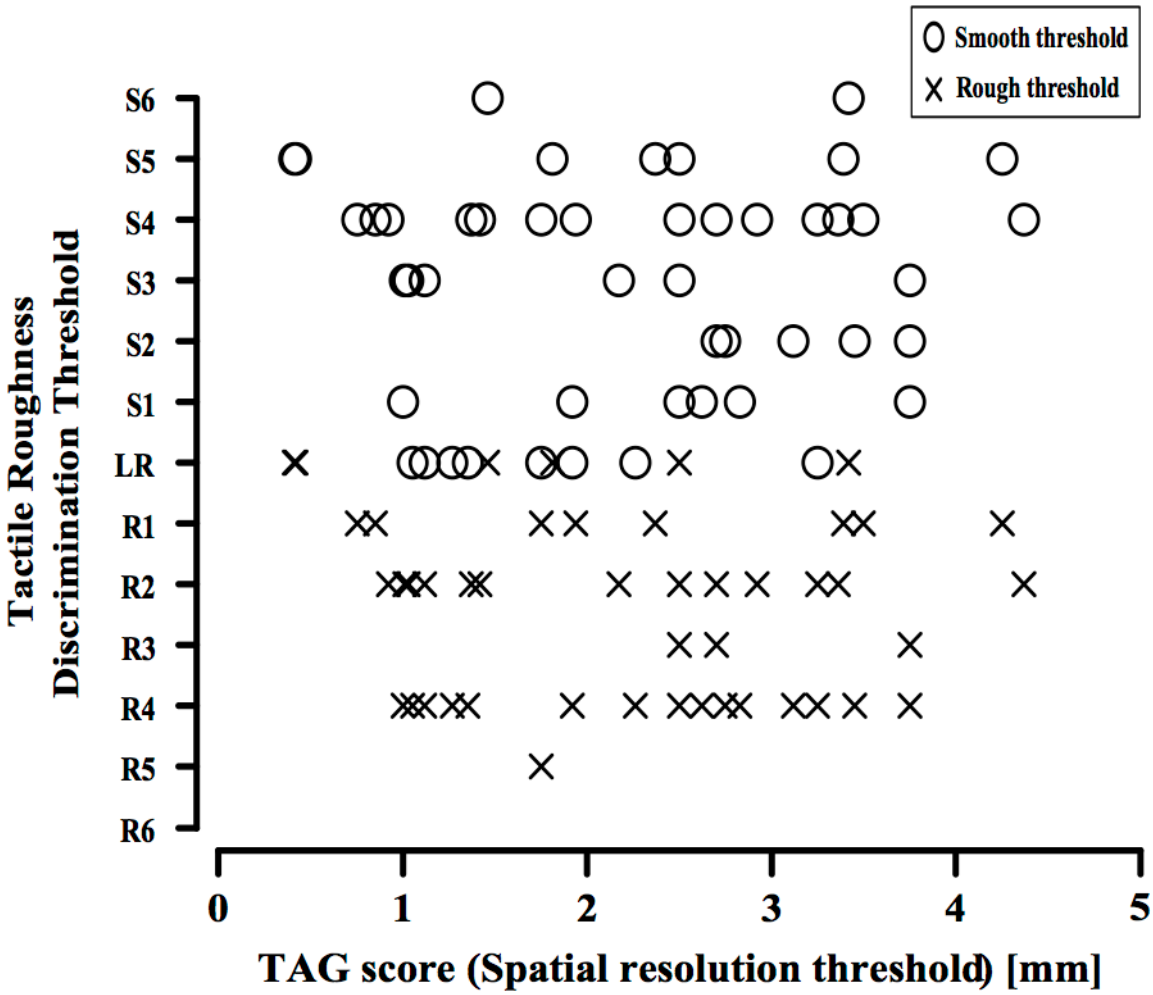

Figure 12: Spatial resolution threshold plotted against tactile roughness discrimination threshold shows no relationship between the two measures. LR represents the limit of resolution.

2.5- Discussion

The present results demonstrated that in a two-forced choice paradigm, subjects showed a lower discrimination threshold (TRDT) with a set of smooth sandpapers than with rough sandpapers. Performance on these tasks was independent of movement related variables such as normal force, tangential force and average scanning velocity exerted by the fingertip against the sandpapers. Performance was also unaffected by gender or age. In contrast, we found that tactile spatial resolution acuity deteriorated

with age. Lastly, there was no significant within-subjects relationship between roughness discrimination and spatial resolution acuity performance.

One goal of the present study was to investigate a new device enabling the determination of an active tactile roughness discrimination threshold at the index fingertip and to characterize the lateral scanning movement in terms of force and velocity. We chose a two-forced choice procedure implemented in a double interlaced staircase method. This procedure has been demonstrated to be highly effective with little interdependence between series. When questioned, all subjects asserted that they perceived that the stimuli were presented in random order. One disadvantage of the device is maintaining consistency between the steps in particle size. While step size in sound and light stimuli is easy to determine and control, a constant step-size in roughness is more difficult to obtain. The average size of the abrasive particles in the sandpapers we used in the present study was specified by the manufacturer (i.e., the "micron grade"). However, the mean spacing between particles is approximately 3 times the grit size (Connor et al., 1990) (54 μm for the finest and 580 μm for the coarsest sandpaper used in the present studies). In other words, spacing is dependent on grit size. Jansson [15] found that the perception of roughness increases with inter-particle spacing. As pointed out by Hollins and Risner (Hollins and Risner, 2000), sandpapers vary from one another not only in particle size, but also particle shape, the material from which they are made and by attachment to the substrate. As a consequence, the stimulus structure of sandpapers is stochastic in nature, making conclusive interpretations more difficult. In future studies, machine-etched surfaces with well-defined spatial periods may serve as a better alternative to sandpaper.

The scores of the TSRT presented in table 3 agree with those previously reported (Bleyenheuft et al., 2006; Sathian and Zangaladze, 1996; Sathian et al., 1997; Tremblay et al., 2003; Van Boven et al., 2000; Vega-Bermudez and Johnson, 2004). In addition, the age dependent decrease in TSRT found in the present study is also in agreement with previous studies. For instance, Bleyenheuft et al. (Bleyenheuft et al., 2006)reported a median and interquartile range for TSRT of 1.2 [1.0-1.8] and 1.1 [0.7-1.4] mm for subjects between 6-9 and 10-16 years of age, respectively. In age groups of 60-71 and 74-95 years of age, Tremblay et al. (Tremblay et al., 2003) found a TSRT of 2.7 ±0.6 and 3.4 ±0.4 mm, respectively. Psychophysical and neurophysiologic studies (Gibson and Craig, 2002; Johnson and Phillips, 1981; Sathian et al., 1989; Yoshioka et al., 2001)have

shown that the TSRT is closely related to the density of slow adapting type 1 (SA1) afferent innervation. Additionally, SA1 receptor density decreases with age (Besne et al., 2002). Together, these findings readily explain the degradation of TSRT performance with age.

It has been shown repeatedly that humans use the SA1 mechanosensitive afferent system to judge the roughness of textures (Johnson and Hsiao, 1992; Sathian et al., 1989; Yoshioka et al., 2001). Yoshioka et al. (Yoshioka et al., 2001)further asserted that spatial variation in SA1 firing rates is the only neural code that accounts for the perceived roughness of surfaces with finely and coarsely spaced elements. However, in an elegant series of experiments, Hollins et al. (Hollins et al., 2002; Hollins and Bensmaïa, 2007; Hollins and Risner, 2000) demonstrated that the perception of roughness for fine textures with a spatial period of less than 100 μm involves high frequency vibratory cues, likely mediated by Pacinian afferents. These observations have revived an interest in Katz's theory (Katz and Krueger, 1989) stating that tactile perception of coarse textures depends on a "spatial sense" while tactile perception of finer textures depends on a "vibration sense". Indeed, our results suggest that there is no relationship between TRDT and TSRT performance. In addition, the absence of degradation in TRDT performance with age, while it is clearly present in the TSRT, suggests that these percepts are differently encoded in peripheral afferents. These two facts indicate that the two tactile submodalities rely on different neural mechanisms, i.e. texture discrimination relying more on an intensive coding whereas grating resolution thresholds depend on the spatial structure of afferent signals. The first one requires only minimal peripheral innervation to support perceptual decision, while the second one is critically dependent upon tactile innervation for the resolution of spatial details leading to judgment about groove orientations. Such differences also explain why TRDT was relatively unaffected by age.

In conclusion, the present studies strengthen the theory that the neural mechanisms underlying tactile roughness discrimination for fine textures differ from those involved in spatial resolution acuity at the level of signal transduction and encoding.

Chapter 3: Tactile roughness discrimination of the finger pad relies primarily on vibration sensitive afferents not necessarily located in the hand

Libouton X, Barbier O, Berger Y, Plaghki L, Thonnard JL.

Tactile roughness discrimination of the finger pad relies primarily on vibration sensitive afferents not necessarily located in the hand. Behav Brain Res. 2012 Apr 1; 229(1):273-9.

3.1- Abstract

This study aims to investigate the relative contribution of remote mechanoreceptors to perception of roughness and spatial acuity. We examined two unilateral pathological conditions affecting differently innervation of the index finger: unilateral carpal tunnel syndrome (n=12) and surgically repaired complete traumatic median nerve section at the wrist following surgical repair (n=4). We employed a control condition consisting of ring-block anaesthesia of the entire index in 10 healthy subjects to model pathological denervation of the fingertip. Spatial acuity and the ability to discern roughness were assessed using a grating orientation task and a roughness discrimination task, respectively.

In patients with carpal tunnel syndrome, we observed a significant reduction of spatial resolution acuity but an intact ability to discriminate roughness with the fingertip.

For patients with traumatic median nerve section there was no recovery with the grating orientation task up to 20 months post surgery but a progressive and full recovery with the roughness discrimination task between 6-9 months.

Finally, in the anaesthetic ring bloc group, the nerve block completely disrupted performances in grating orientation task, but unexpectedly left unaffected performances in the roughness discrimination task.

Taken together, these lines of evidence support the view that the neural mechanisms underlying tactile roughness discrimination differ from those involved in spatial

resolution acuity. Vibrotaction is necessary and sufficient for the perception of fine textures and, when the innervation of the fingerpad is compromised, information about textures can be captured and encoded by remote mechanoreceptors located in more proximal tissues where the innervation is intact.

KEY WORDS: Tactile roughness perception, Spatial resolution acuity, vibrotaction, fingertip.

3.2- Introduction

In a recent paper (LIBOUTON et al., 2010), we showed that there was no significant within-subjects relationship between tactile spatial resolution threshold and tactile roughness discrimination threshold and inferred that the two tactile sub modalities rely on different neural mechanisms, with grating resolution threshold seeming to depend on the spatial structure of afferent signals and roughness discrimination seeming to rely more on intensity coding. Tactile spatial resolution threshold is critically dependent upon tactile innervation for resolution of spatial details needed to make judgments concerning groove orientation, whereas tactile roughness discrimination threshold requires only minimal peripheral innervation to support perceptual decision-making.

Psychophysical and neurophysiologic studies have demonstrated spatial resolution acuity in glabrous skin to be closely related to the density of Merkel neurite complexes associated with slowly adapting type 1 (SA1) fibers (Gibson and Craig, 2002; Johnson and Phillips, 1981; Sathian et al., 1989; Yoshioka et al., 2001). Several investigators have proposed that this SA1 mechanosensitive afferent system may also be involved in the tactual perception of texture roughness (Johnson and Hsiao, 1992; Sathian et al., 1989; Yoshioka et al., 2001). Yoshioka et al. (2001) postulated that spatial variation in SA1 firing rates was the only neural code that could account for the perceived roughness of surfaces with finely and coarsely spaced elements. With an elegant series of experiments, Hollins et al (Hollins et al., 2002; Hollins and Risner, 2000) revived interest in Katz's theory (Katz and Krueger, 1989) arguing that tactile perception of coarse textures depends on a "spatial sense" while tactile perception of

finer textures depends on a “vibration sense”. They formulated a duplex theory of roughness wherein roughness is thought to be mediated by two neural codes. Accordingly to their theory, coarse textures (with spatial periods ≥200 μm) are encoded by SA1 mechanoreceptors while tactile perception of finer textures are encoded by Pacinian (FAII) and Meissner (FAI) corpuscles responding to cutaneous vibrations generated by the scanning of textures with the fingertips (Bensmaïa and Hollins, 2005; 2003; Hollins Sliman J Bensmaïa Sean W, 2001; Hollins and Bensmaïa, 2007; R. S. Johansson and Flanagan, 2009; Yoshioka et al., 2001). However, the thesis asserted by Hollins and Risner(Hollins et al., 2002) was strongly refuted by Yoshioka et al. (2001) as they postulated that spatial variation in SA1 firing rates was the only neural code that could account for the perceived roughness of surfaces with finely and coarsely spaced.

The aforementioned studies were performed employing direct touching of textured surfaces with the fingertips. However, Klatzky and collaborators demonstrated that it is possible to perceive texture roughness by indirect touch through a rigid probe (Klatzky and Lederman, 1999; Klatzky et al., 2003). Although, several investigators have reported subtle differences between direct and indirect touch (Hollins and Bensmaïa, 2007; Hollins et al., 2004; Yoshioka et al., 2007), studies employing indirect touch paradigms have underscored the importance of vibrotactile coding in tactile perception of roughness.

The Pacinian and Meissner corpuscles are generally thought to be the primary receptors mediating detection of cutaneous vibrations. The Meissner corpuscles are distinguished from the Pacinian corpuscles by their much smaller receptive field and by being most sensitive to vibratory stimuli in the range from 40 Hz to 60 Hz. The Pacinians are most sensitive in the range from 60 Hz to 400 Hz; they are orders of magnitude more sensitive and because of their sensitivity, their receptive field areas are orders of magnitude larger (Bensmaïa and Hollins, 2005; 2003; Hollins and Bensmaïa, 2007; R. S. Johansson and Flanagan, 2009; R. S. Johansson and Vallbo, 1979; Yoshioka et al., 2001). Pacinian corpuscles are abundant in the dermis and subcutaneous tissue beneath the glabrous skin of the hands, in the aponeuroses and tendon sheaths of skeletal muscle, around ligaments, in fascial planes, in the periosteum and interosseous membranes, and in muscle tissue itself (Mountcastle, n.d.). Moreover, multiple lines of evidence have shown that high frequency vibratory disturbances are transmitted readily through

cutaneous and subcutaneous tissues, including results of analysis of the visco-elastic properties of these tissues (Moore, 1970) and the common observation in electrophysiological experiments that the Pacinian channel can be activated by transient mechanical disturbances, often quite remote from the receptor location (Vallbo and R. S. Johansson, 1984). Furthermore, Morley et al. (Morley et al., 1988) observed that following a lesion of the lateral digital nerve innervating the terminal phalanx of the left index finger, a patient was able to detect vibration across a wide range of frequencies, reflecting the spread of the vibratory stimulus through the skin and the spatial characteristics of functionally intact receptor/afferent groups innervating neighboring skin (Nelson, 2010).

Given that, by their very nature, vibrations generated at the interface of textured surfaces with the fingertip propagate proximally through the finger towards the hand and forearm, and since all these tissues contain highly mechanosensitive receptor afferents able to encode vibrations, we were prompted to investigate the relative contribution of the remote mechanoreceptor afferents to tactual perception of roughness and spatial acuity. Thus, we examined two unilateral pathological conditions affecting differently innervation of the index finger: unilateral carpal tunnel syndrome and surgically repaired complete traumatic median nerve section. Electrodiagnostic studies performed to follow the recovery of the patients suffering from traumatic median nerve section are described in the supplemental text and the associated data are presented in Table S1. And we employed a control condition consisting of ring-block anesthesia of the entire index finger in healthy subjects to model pathological denervation of the fingertip. Spatial acuity and the ability to discern tactual roughness were assessed using a grating orientation task and a tactile roughness discrimination task, respectively, as illustrated in Figure 13.

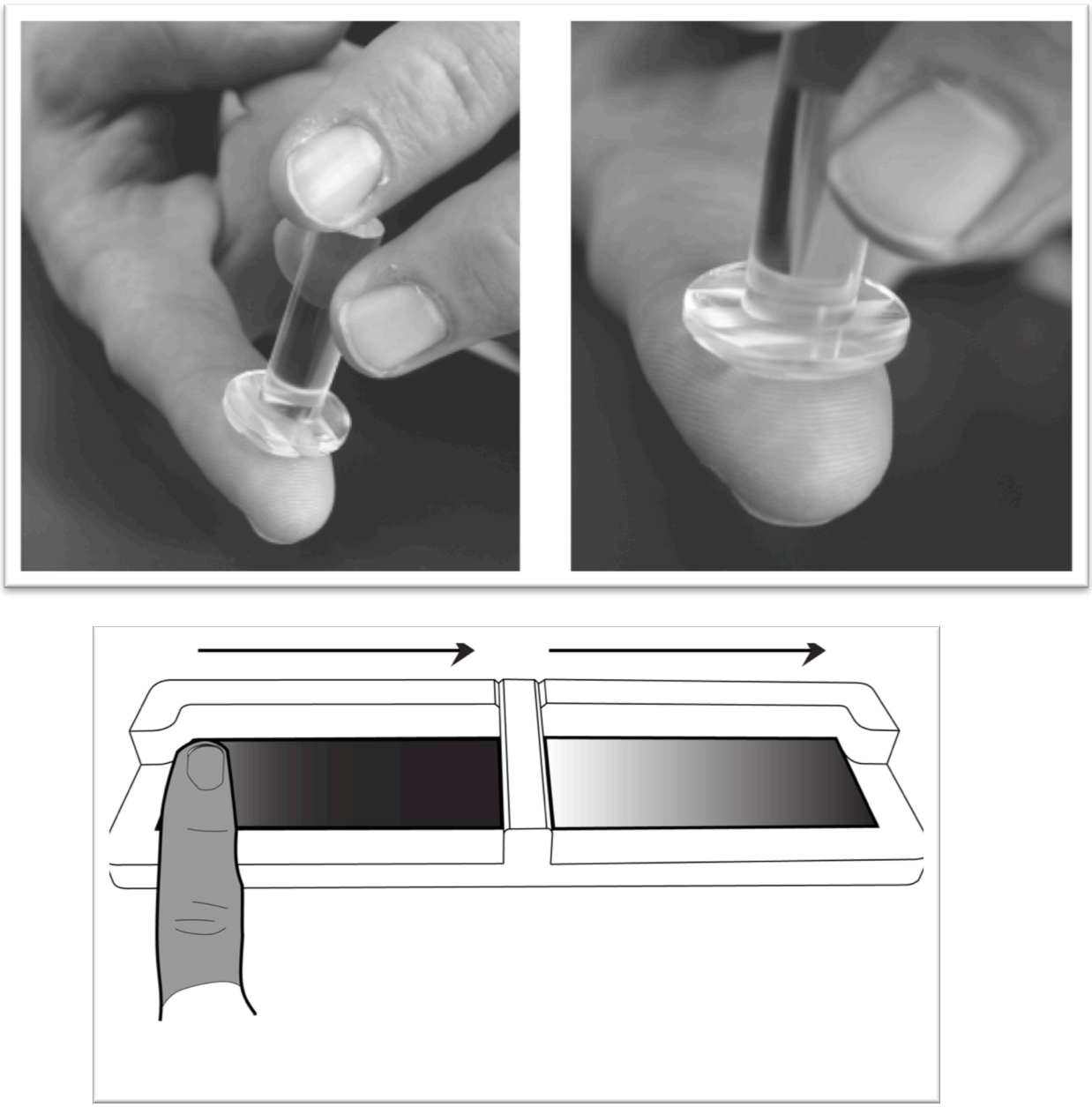

Figure 13: Sensory assessments. (A) Photographs of a grating orientation task stimulus in use. (B), Illustration of tactile roughness discrimination task apparatus in use.

3.3- Materials and methods

3.3.1- Subjects

Written informed consent forms were obtained from all participants. The Ethics Committee of the *Université catholique de Louvain ("Commission d'éthique biomédicale hospitalo-faculatire")* approved all of the experimental procedures. All participants were tested using two sensory assessments, as described below.

Three groups of participants took part in the present study. The first group, termed CTS, consisted of 12 patients (6 males, 6 females; 66 ±14 years of age) who were suffering from unilateral CTS, recruited consecutively at the Hand Surgery Unit of our institution (Cliniques universitaires St. Luc, Brussels, Belgium). To be eligible, the patients had to fulfill the diagnostic criteria for CTS according to the American Academy of Neurology {Jablecki:2002hx}. These criteria are pain, paresthesia, swelling, clumsiness or weakness of the hand, sensory deficits in the median innervated region of the hand, hypotrophy or motor deficit of the median innervated thenar muscle, and positive Phalen test result (considered to be positive when a 1-min passive forced flexion of the wrist elicits symptoms). A detailed clinical history, a careful clinical examination and an extended neurophysiologic evaluation (electromyographic, nerve conduction velocity, and compound action potential recordings) were performed to exclude the presence of other diseases. Only patients with CTS without etiologic factors (Giannini et al., 2002)were included in this study.

The second group, termed TRA-SEC, consisted of 4 patients (3 males, 1 female; 53 ±17 years of age) suffering from a complete traumatic median nerve section at the wrist. These patients were treated by a microsurgical suture of the nerve lesion. Due to the anatomical position of the median nerve, all patients presented also a section of the wrist and finger flexor tendons. The tendons were sutured concomitantly with the median nerve. The procedure was performed in the Hand Surgery Unit of our institution by O.B. The patients were evaluated 1 wk, 3 mos., between 6 and 9 mos., and ≥1.5 y after their operations. Electrodiagnostic studies were also performed at month 6 and between

months 15 and 20 after post-injury. The findings of those electrodiagnostic studies are described in the supplemental text and Table S1.

The third group, termed AN-BLOC, consisted of 10 healthy volunteer subjects

(10 males, 31 ±11 years of age). All of them were free from diseases and injuries that could have affected the tactile sensitivity of their hands. The digital nerves at the base of the index finger were blocked by four injections of 2% xylocaine (Astra-Zeneca®) to achieve a ring-block anesthesia of the entire index finger (Augurelle, 2002). Clinical anesthesia was obtained when all sensations were abolished as indicated by complete insensitivity to skin contact with the Semmes Weinstein monofilaments (Lafayette Instrument) (Bell-Krotoski and Tomancik, 1987; Bell-Krotoski et al., 1993; 1995).

3.3.2- Grating orientation task

The grating orientation task was carried out using JVP Domes (JVP Domes, Stoelting Co., Wood Dale, IL) on the index finger of the affected hand. The test kit included a serial set of eleven hemispherical plastic dome gratings having equidistant bar and groove widths at the following widths (in mm): 0.35, 0.50, 0.75, 1.00, 1.20, 1.50, 2.00, 3.00, 3.50, 4.00, and 4.50. Each dome was applied perpendicularly to the skin for approximately 2 s with a skin indentation of 1–2 mm (Fig. 11). The domes were randomly aligned in one of the two orthogonal directions (i.e. with the grooves parallel or transverse to the long axis of the index finger). Blindfolded subjects were required to identify the stimulus orientation before the stimulus was removed. A procedure adapted from that of Van Boven and Johnson was used (Bleyenheuft et al., 2006; Van Boven and Johnson, 1994b). The 3-mm grating was first applied for 10 consecutive trials using a randomized orientation of the bars. If the subject succeeded with the 3-mm grating, then the next smaller grating (2 mm) was applied and so forth. The test was stopped when the percentage of correct answers for the grating reached 50%. If the subject failed at the 3-mm grating, the next larger grating (3.5 mm) was applied. The test pursued with larger gratings until the subject reached a score higher than 75% of correct answers. A simple linear interpolation estimate of the 75% correct grating width was taken as the tactile spatial

resolution threshold value. A lower tactile acuity grating score (TAG score) signified better tactile spatial resolution acuity.

$$TAGscore = g_{below} + \frac{0.75 - p_{below}}{p_{above} - p_{below}}(g_{above} - g_{below})$$

Where g = grating width of a probe, p = probability of correct answers, *above* = the grating width that results in a score closest to but above 75% correct, and *below* = the grating width that results in a score closest to but below 75% correct.

3.3.3- Tactile roughness discrimination task

The tactile roughness discrimination task has been explained in detail elsewhere (LIBOUTON et al., 2010)1. Briefly, each subject was comfortably seated at a table facing the experimenter and was requested to position the index finger of the dominant hand just in front of two textured surfaces, each with an area of 7.5 × 3.0 cm (Fig. 13). A cardboard screen was placed over the participant's wrist to block visibility of his or her hand. Without further instructions, the participant was asked to slide the fingertip of their index finger on the first stimulus (located on the left side) and then subsequently on the second stimulus (located on the right side). After each trial, the participant was asked to discriminate the textures by reporting which was the rougher surface. Between trials, the subject raised his or her index finger to allow the experimenter to reposition it on the left side for the presentation of the next stimulus. The subjects scanned each stimulus with a single sweep using their naturally applied contact force and scanning velocity. The subjects wore sound attenuating headphones to muffle any extraneous noise.

Table 4. Set of sandpapers used as stimuli in the tactile roughness discrimination task.

Surface	Stimulus N°	FEPA P-grade	Average grit size (μm)	Threshold
Smoothest	13	P1000	18	S6
	12	P800	22	S5
	11	P600	25.8	S4
	10	P500	30	S3
	9	P400	35	S2
	8	P360	40	S1
Reference	7	P320	46	LR
	6	P240	58	R1
	5	P220	65	R2
	4	P180	78	R3
	3	P120	127	R4
	2	P100	156	R5
Roughest	1	P80	195	R6

Thirteen pieces of sandpaper (see Table 4), with average grit sizes varying from 18 µm (grit number P1000, the finest stimulus) to 195 µm (grit number P80, the coarsest stimulus) were used as stimuli. Grit number and particle size ("micron grade") are described in accordance with the Federation of European Producers of Abrasive Products (FEPA) P-grading system.

Two tactile roughness discrimination thresholds (one for rough and one for smooth surfaces) were determined using a double interlaced adaptive staircase procedure based on a two-alternative forced choice paradigm. The tactile roughness discrimination threshold was defined as the amount of change required to produce a 75% just noticeable difference (75%jnd) in sensation. The stimulus difference was defined as the difference in particle size between a given stimulus and the reference stimulus (P320). If subjects were able to discriminate correctly the smallest difference in particle size (P240 and/or P360 vs. reference P320), their discrimination performance exceeded the limit of resolution of the stimuli. For these subjects, we allowed a threshold value of half the smallest difference in particle size.

3.3.4- Statistics

Paired t-tests were used to compare the thresholds elicited for the unaffected versus the affected hand of all participants to this study. Non-parametric statistics were applied when normality tests failed or when statistics were performed on ordinal data. The level of significance for the P value was set to 0.05.

3.4- Results

3.4.1- Spatial acuity performance in the grating orientation task

As shown in Figure 14, a significant reduction in tactile spatial resolution ability in the grating orientation task was observed in the affected hand of CTS patients, relative to the unaffected hand, as evidenced by all tactile acuity grading scores of the patients' affected hands being located above the identity line of the equality plots (paired *t*-test, $t = -2.21$; $p < 0.05$). Grating orientation task performance was measured at four different periods in TRA-SEC patients: within the 1st week (T0), 3 months (T1), 6–9 months (T2), >18 months (T3). The most dramatic finding for the TRA-SEC group was that the patients were unable to perceive grating orientation on the index finger pad of the affected hand for more than 18 months postoperatively. Of note, and as already reported in the literature (Bleyenheuft and Thonnard, 2007), the reproducibility of the grating orientation task for the unaffected hand was very high across the four time points ($p>0.5$). The mean tactile acuity grading score was 2.15 mm (± 0.72 mm) in the normal subjects (age 31±11) but after anesthetic block of their fingers, they were all completely unable to perform the task.

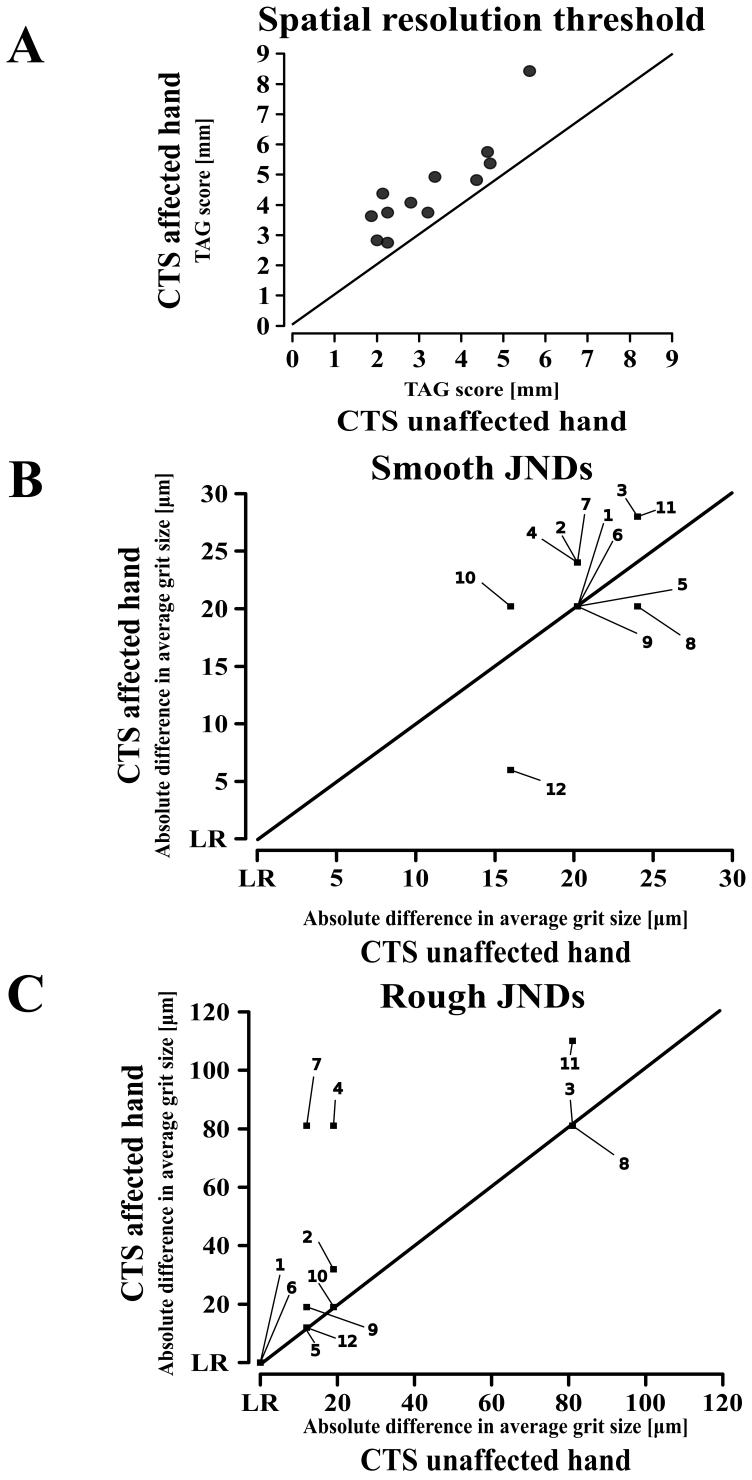

Figure 14: Patients with unilateral Carpal Tunnel Syndrome (CTS). (A) Tactile spatial resolution thresholds in TAG scores for unaffected vs. affected hands. (B & C) Just Noticeable Differences (JNDs) in tactile roughness discrimination thresholds with smooth stimuli (B) and rough stimuli (C) in unaffected vs. affected hands. The 75% JNDs are expressed as the absolute difference in the average grit size between a given sandpaper and the reference sandpaper (P320; see Table 1), where LR represents the Limit of Resolution. The line in each graph represents the "identity line".

3.4.2- Roughness discrimination performance

In subjects with the carpal tunnel syndrome, there was no difference in roughness discrimination between the affected and non-affected hand for either smooth or rough stimuli (Fig. 14 Wilcoxon's paired ranked test, $p>0.05$ for both). The TRA-SEC patients' performance data for rough and smooth textures in the tactile roughness discrimination task for the same four postsurgical time periods described above are shown in Figure 15. During the first week post surgery (T0), all TRA-SEC patients had no ability to perceive roughness when scanning the sandpapers with the index finger pad of the affected hand. Three months after surgery (T1), some patients were able to discriminate a couple of the roughest sandpapers. During the 6 to 9-mo. time period (T2), both the smooth and rough tactile roughness discrimination thresholds measured on the index finger pad of the affected hand became similar to those in the unaffected hands. It should be noted that we observed excellent reproducibility of the tactile roughness discrimination test results across the four different time periods for the index finger pads on the patients' unaffected hands. Finally, as shown in Figure 16, the anesthetic ring bloc had no effect on smooth or rough tactile roughness discrimination thresholds in the AN-BLOC group (Wilcoxon's paired rank test, $p = 0.10$ and $p = 0.46$, respectively). In fact, most (8/10) of the AN-BLOC participants reported spontaneously that they could feel vibrations but could not characterize the un/pleasantness of touch sensations while under anesthetic block.

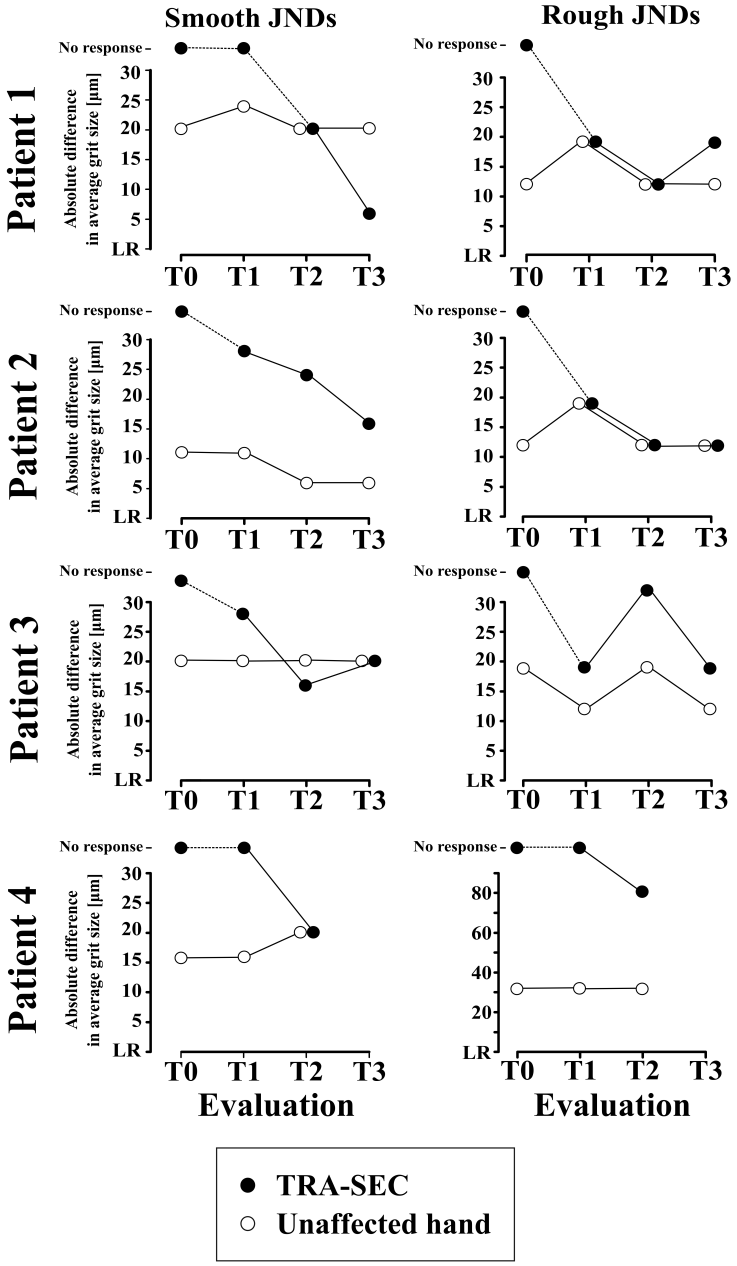

Figure 15: Patients with a unilateral traumatic sectioning of the median nerve and wrist flexor tendons (TRA-SEC). Just Noticeable Differences (JNDs) in tactile roughness discrimination thresholds with smooth stimuli (left column) and rough stimuli (right column) in unaffected (open circles) vs. affected (black circles) hands. The 75% JNDs are expressed as the absolute difference in the average grit size between a given sandpaper and the reference sans paper (P320; see Table 1), where LR represents the Limit of Resolution. Patients were evaluated four times (except patient 4 who was evaluated three times) during the post-surgical period, i.e., at 1 wk (T0), 3 mos. (T1), between 6 and 9 mos. (T2), and ≥1.5 years (T3).

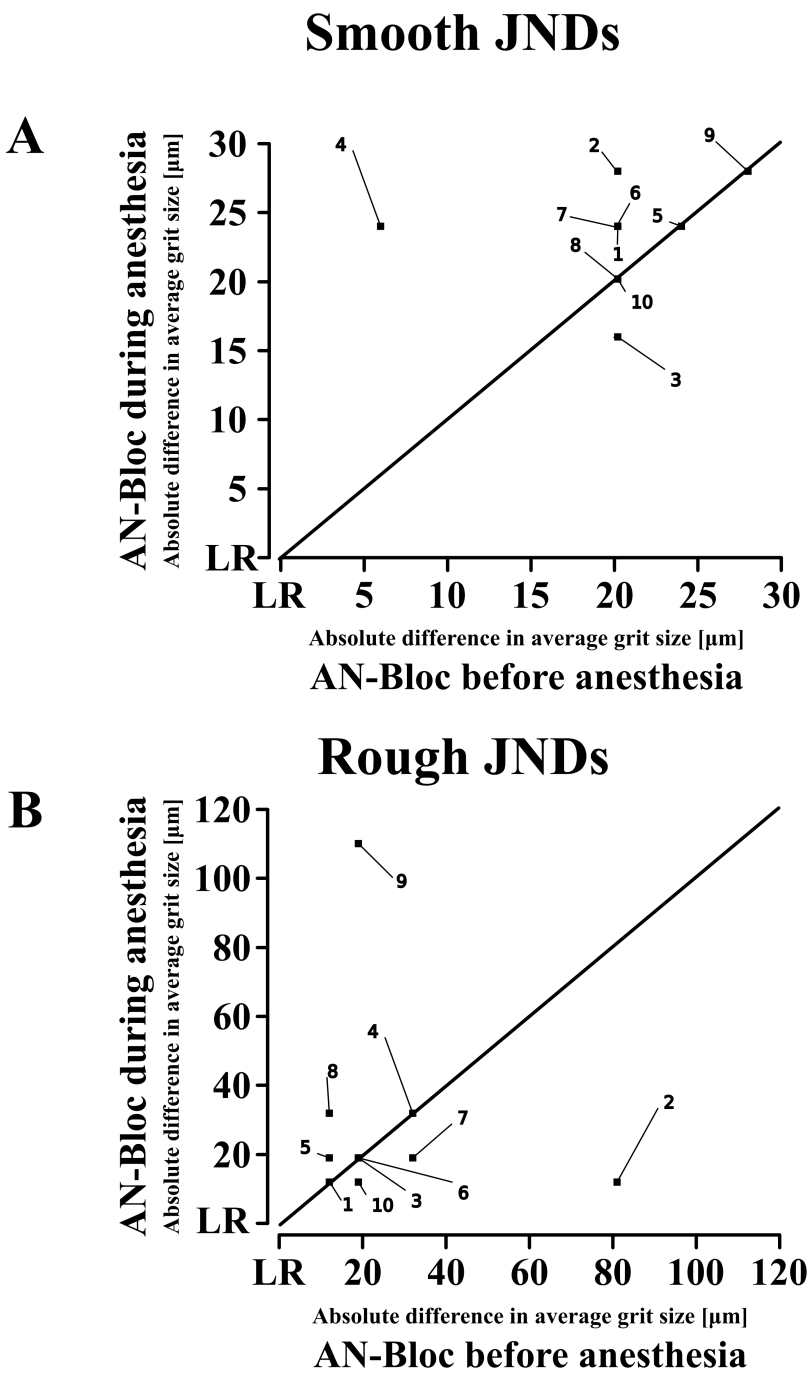

Figure 16: Subjects with anesthetic ring bloc of the index finger (AN-BLOC). Just Noticeable Differences (JNDs) in tactile roughness discrimination thresholds with smooth stimuli (A) and rough stimuli (B) before and during anesthesia. The 75% JNDs are expressed as the absolute difference in the average grit size between a given sandpaper and the reference sans paper (P320; see Table 1), where LR represents the Limit of Resolution. The line in each graph represents the "identity line".

3.5- Discussion

In the present study, we found that patients with CTS had a significant reduction of spatial resolution acuity while maintaining an intact ability to discriminate roughness with their fingertips. On the contrary, tactile roughness discrimination performance was unaffected by entrapment of the median nerve. The TRA-SEC patients exhibited no performance recovery in the grating orientation task for up to 20 months postoperatively, but did show a progressive and nearly full recovery in their tactile roughness discrimination performance by 6–9 mos. postoperatively (T3). Finally, in the AN-BLOC subjects, who were given an anesthetic ring bloc in the absence of any pathology, we observed disrupted grating orientation performance in the absence of any apparent effects on their ability to perform the tactile roughness discrimination task.

Taken together our results showed that the neural mechanisms underlying the tactile roughness discrimination differ from those involved in spatial resolution acuity. Remarkably, our findings provide some evidence that roughness discrimination rely primarily on vibration sensitive afferents not necessarily located in the hand. This dissociation raises several questions. Firstly, how are the physical properties of tactile stimuli, produced at the finger pads in contact with the material, conducted to sensory structures remote from the finger pads? Further, where and how is information related texture encoded and conveyed to the central nervous system.

Similar subjective roughness magnitudes are obtained when textured surfaces are actively scanned indirectly with a rigid probe or directly with the finger pad, indicating that vibrations generated at the interface of the probe with textured surfaces carries the critical information needed for roughness discrimination (Brydges et al., 2005; Klatzky et al., 2003; Klatzky and Lederman, 1999). Moreover, performance on the tactile roughness discrimination task employed here is independent of variables such as normal force, tangential force, and average scanning velocity (LIBOUTON et al., 2010). Consequently, we can surmise that the fully anesthetized index finger may act like a probe, transmitting the biophysical interaction of the finger pad with external stimuli to remote tactile sensors that are capable of encoding this information. This line of reasoning can also be applied to explain the dissociated abilities observed in the CTS

group. Indeed, the numbness and loss of the sensory nerve responsivity experienced by CTS patients is thought to be due to entrapment of the median nerve in the carpal tunnel leading to pathophysiological changes such as decreased nerve conduction velocity in large myelinated fibers (Werner and Andary, 2002). Presumably, the presently reported grating orientation task performance deficit in CTS patients also reflects these physiopathological changes. The absence of a deficit for the CTS patients in roughness discrimination performance may be analogous to the intact roughness discrimination performance we observed in our control subjects while they had an anesthetic digit bloc. That is, the biophysical information related to material roughness may be transmitted to remote receptors while the anesthetized index finger or the finger of a CTS-affected hand acts as a probe. These observations are concordant with those of Morley et al. (Morley et al., 1988)who reported an increase in vibratory detection threshold for low frequencies (5–40 Hz) and unchanged detection of high frequencies (80–250 Hz) following a lesion of the lateral digital nerve innervating the terminal phalanx of the left index finger. In their interpretation of these findings, Morley and colleagues suggested "the differential effect of the nerve lesion on vibratory thresholds reflects the spread of the vibratory stimulus through the skin and the spatial characteristics of functionally intact receptor/afferent groups innervating neighboring skin". It is interesting to underline here that the detection of 'flutter' elicited by frequencies between 5 H and 40 Hz is mediated by activity in the FA I units reflecting the importance of these units for extracting spatial features of dynamic mechanical events such as scanning across a textured surface.

The present findings have important implications with respect to where and how the biophysical information concerning textured surfaces is encoded and conveyed to the central nervous system, particularly when sensors in the fingertips are bypassed as a result of a nerve block or peripheral neuropathy. Our results suggest that vibrations travel to remote skin locations where the innervation is intact, and that remote mechanoreceptors (most probably Pacinian afferents) would mediate residual roughness discrimination. Indeed, Delhaye et al (2010) (Delhaye et al., 2012) observed that non-periodic vibrations generated at the index fingertip when scanning sandpapers were readily transmitted to the wrist and forearm. The frequency content of the vibration did not enable to discriminate the different stimuli. However, the intensity of the signal was a good candidate to code the roughness of the texture.

As noted in the Introduction, textures with spatial periods greater than ~200 μm are encoded by SA1 receptors in the finger pads, whereas roughness discrimination of finer textures (spatial scale <200 μm) is mediated by the encoding of cutaneous vibrations generated during scanning movements. The Pacinian afferents, which are the primary receptors that encode these cutaneous vibrations (Bensmaïa and Hollins, 2005; 2003; Hollins and Bensmaïa, 2007; R. S. Johansson and Flanagan, 2009; Scheibert et al., 2009; Yoshioka et al., 2001), are present in the subcutaneous layer of the skin but are also observed near tendons, periarticular, and interosseus ligaments and muscles (Mountcastle, n.d.). It is perhaps worthwhile to recall Hunt and McIntyre's (Hunt and McIntyre, 1960a; 1960b; 1960c) discovery of very sensitive rapidly-adapting vibration receptors in the interosseus nerve of the hind limb in cats that responds to vibrations transmitted through the foot pad "almost like a seismograph". Hunt (Hunt, 1961) characterized them as Pacinian corpuscles with a sensitivity so great that very small vibrations transmitted through the skin and soft tissues, even applied at a considerable distance, readily evoked vigorous discharges. Jozsa et al. (Jozsa et al., 1988) found that all of the known types of mechanoreceptors were present in the myotendinous junctions of human palmaris longus muscles. Pacinian corpuscles were observed frequently on the tendineal side, but rarely on the muscular side. In turn, Golgi tendon organs were observed frequently on the muscular side, but rarely on the tendineal site. They found that receptors were distributed homogeneously in both the muscle and tendon parts of the junction, with a distance at least 250 μm between two mechanoreceptors. Fallon and Macefield (Fallon and Macefield, 2007) showed that the response profile to small vibrations of muscle spindle primary and secondary endings overlapped with that of Golgi tendon organs (20–120 Hz). They further demonstrated that these three receptor types had similar thresholds when stimuli were delivered to the parent muscle's distal tendon, but only during weak voluntary muscle contraction (±5% of maximum voluntary contraction). In other words, Golgi tendon organs (1b afferent fibers) located in the distal tendons could potentially participate in the encoding of vibrations generated during active scanning, employing direct (through the fingertip) or indirect (through a rigid probe) touch of textured objects. It is important to recall here that, when the muscles were completely relaxed, Golgi tendon organs did not respond to vibration. Therefore, it should be possible to study the relative contribution of Golgi tendon organs relative to that of Pacinian corpuscles by comparing roughness

discrimination task performances in active, passive and pseudo-passive scanning trials of textured surfaces using an anesthetic ring block of the index finger with well-controlled wrist positions and voluntary muscle contractions (e.g., ±5% of maximum voluntary contraction according Fallon & Macefield's observations (Fallon and Macefield, 2007)).

Given the aforementioned prior findings, the current results confirm that the neural mechanisms underlying roughness perception for fine textures differs from those involved in spatial resolution acuity (LIBOUTON et al., 2010). Many previous studies (Hollins et al., 2002; Hollins and Bensmaïa, 2007; Hollins and Risner, 2000; LIBOUTON et al., 2010; Yoshioka et al., 2007) have shown that perception of roughness of finer surfaces involves detection of cutaneous vibrations generated when textures move across the skin. When the mechanosensitive afferents from the fingertips are rendered ineffective, such as in our TRA-SEC patients and AN-BLOC subjects, the tactile spatial acuity encoded in the SA1 and FA1 afferents is, as expected, lost completely. However, roughness perception based mainly on vibrations generated at the finger pads is preserved in the absence of functional mechanosensitive afferents in the fingertips since these vibrations are transmitted to remote mechanosensitive transducers located in proximal tissues where the innervation is preserved. During active scanning of textures with the index finger, these remote transducers are sensitive enough to allow normal roughness discrimination ability without any contribution of the mechanoreceptors in the fingertips. Further investigations are needed to evaluate, in normal conditions, the relative contribution of these remote mechanoreceptors to the perception of texture.

Acknowledgments: The authors are grateful to the participants for their kind participation. This research was undertaken within the FP6-NMP NANOBIOTACT project (contract no. 033287) and the FP7-NMP NANOBIOTOUCH project (contract no. 228844).

3.6- Supplemental Text

Due to the anatomic location of the median nerve below the flexor tendons in the wrist, nerve section in isolation is very rare. As a consequence, the flexor tendons surrounding the median nerve are usually severed and must be repaired. This was the case in the 4 TRA-SEC patients in the present study. Furthermore, mobility of the affected hand was limited by a splint during the first 2–3 mos. after surgery to facilitate healing of the median nerve and flexor tendons. Recovery of active motion of the hand and wrist, guided under a physiotherapist's supervision, was achieved 6–9 mos. after the operation. All 4 patients regained the to bend completely the fingers on their injured hands attesting functional recovery of the flexor tendons. Electrodiagnostic studies of the sutured median nerve showed an absence of sensitive response that lasted up to 20 mos. (see Table S1).

Table S1. Electromyographic follow-up studies in TRA-SEC patients.

Patient (affected hand)	6 mos. postoperative				>15 mos. postoperative			
	DMLm (mS)	CMAPm (mV)	DSLm (mS)	SNAPm (mV)	DMLm (mS)	CMAPm (mV)	DSLm (mS)	SNAPm (mV)
1 (R)	NR	NR	NR	NR	9.1	0.4	NR	NR
2 (R)	NR	NR	NR	NR	NE	NE	4.5	5
3 (L)	NR	NR	NR	NR	NE	NE	3.6	6
4 (R)	NR	NR	NR	NR	///	///	///	///
Norms	<4.4	>4.0	<3.5	>20	<4.4	>4.0	<3.5	>20

Distal peak sensory latencies (**DSLm**) and sensory nerve action potential amplitudes (**SNAPm**) of the median nerve were recorded at the index finger after stimulation 13 cm proximally at the wrist. The distal motor latencies (**DMLm**) and compound muscle action potential (**CMAPm**) of the median nerve were recorded from the abductor pollicis brevis muscle after stimulation 7 cm proximally at the wrist. **R**, Right ; **L**, Left ; **NE**, Not evaluated; **NR,** No Response; ***///,*** Patient lost to follow up.

Chapter 4: Conclusion and perspectives

4.1 Main findings and new hypotheses

We developed a new instrument for determining roughness discrimination threshold and showed that data obtained with it were specific to roughness discrimination and unrelated to tactile spatial acuity. Moreover, it was shown that ring-finger block anesthesia disrupted performance in a grating orientation task completely but, unexpectedly, did not affect performance in the roughness discrimination task. These results support the view that the neural mechanisms underlying tactile roughness discrimination differ from those involved in spatial resolution acuity. Indeed, vibrotaction is necessary and sufficient for the perception of fine textures. Moreover, when innervation of the fingerpad is compromised (e.g., from nerve transection at the wrist), information about textures can be captured and encoded by remote mechanoreceptors located in more proximal tissues with intact innervation. These results led us to formulate new questions and hypotheses.

First, it is commonly accepted that there are four types of mechanoreceptors innervating the glabrous skin of the hand. In a series of review papers, Johnson (Johnson, 2001; Johnson et al., 2000; Johnson and Hsiao, 1992) ascribed a different perceptual function—shape and texture; motion; skin stretch; and vibration—to each type of afferent. This notion was challenged previously by Saal et al. (Saal and Bensmaïa, 2014). We showed that roughness perception remains unaffected in the absence of direct sensory afferent information from the fingerpad. Our findings provide evidence suggesting that roughness perception can rely on vibration-sensitive afferents that are not necessarily located in the finger. This unexpected observation raises a number of significant issues, such as: what is the identity of these other sensitive afferents, where are they located, and is vibration perception sufficient to estimate roughness?

Second, we observed that tactile spatial resolution threshold was unrelated to tactile roughness discrimination threshold. In addition, patients who suffered a traumatic nerve section were unable to perceive grating orientation on the finger pad of the affected hand for more than 18 months after the section was repaired surgically, but

experienced a complete recovery of roughness perception within 6 to 9 months of the repair surgery. Due to the anatomical location of the median nerve in the wrist, traumatic sections of the median nerve never occur in isolation; flexor tendons are damaged concomitantly in cases of median nerve section. Recovery of active flexion of the fingers seems to be crucial to regaining roughness discrimination ability. This need for active flexion points to a fundamental role of tendons in roughness perception of roughness. We hypothesize that fine texture perception tendons may act as strings conveying cutaneous vibrations generated at the fingertips by scanning movements to more proximally located sensory organs.

We had the opportunity to evaluate the functional recovery of a monolateral hand transplanted patient. The results are not yet published. Interestingly, while the tactile spatial resolution threshold, the tactile pressure detection threshold and the digital dexterity were severely compromised, the roughness discrimination threshold of the transplanted hand remained unaffected compared to the contralateral hand. These results confirm that roughness discrimination can be coded by some receptors located in the forearm.

In a very interesting study, Yoshioka et al. (Yoshioka et al., 2011) reported that, despite fluctuating sensory inputs transmitted from the finger, a brick surface feels rough regardless of how slowly or rapidly one's fingers are moved across its surface. Moreover, cutaneous afferents, considered to be critical mediators of roughness perception, are sensitive to scan velocity and contact force which is not compatible with the above observation.

To account for this sensitivity, Yoshioka and colleagues introduced the concept of "**roughness constancy**", defined as:

> *…a special case of roughness perception in which the perceived roughness rating is constant for a particular surface regardless of scanning conditions such as varying speed or contact force*.

Their studies focused on the central question of how roughness constancy is achieved.

In active touch, subjects obtain additional information from their motor efference representation of the desired hand movement as well as proprioceptive information about the position and speed of their hand's movement. Yoshioka et al. (Yoshioka et al., 2011) designed a new concept of hand movement called pseudo-passive scanning

wherein the experimenter moves the subject's hand, providing the subject with proprioceptive input in the absence of a motor efference copy of the movement. Under these conditions, perceived roughness ratings were constant. They concluded that cutaneous input provides the signals that are necessary for roughness perception and that roughness constancy is dependent upon proprioceptive input resulting from hand movement rather than a motor efference copy.

Considering our findings in patients with a traumatic nerve section in the context of Yoshioka and colleagues' findings emphasizes the role of proprioception in modulating sensory information in roughness perception. These findings also suggest that the somatosensory system is able to collect textural information from sources other than fingertip afferences. Delhaye et al. (Delhaye et al., 2012) studied the vibrations generated during the scanning of textured surfaces. They showed that the vibratory waves produced by scanning movements propagate at least to the wrist.

Although Pacinian corpuscles are good candidates for the encoding of vibratory intensity, the physiology underlying vibratory encoding remains unclear. Note that, in our study reported in chapter 3 (fig. 15), roughness perception at T0 (the week following surgery) was completely abolished even for very rough and smooth surfaces. However, from T1 (3 months after surgery) on, roughness perception was possible. Between T0 and T1, there was recovery only of the kinematic function of the patient's index finger. As mentioned by Delhaye et al. (Delhaye et al., 2012), biomechanical properties of hand tissues allow surface interaction signals to be transmitted far away from the contact area into the forearm. In light of these findings, it seems realistic to propose that receptors (cfr. Introduction, point 2) usually implicated in proprioception could have a more important contribution than suspected. They could be implicated in roughness perception.

To my knowledge, median nerve section is the only clinical condition in which roughness perception is completely abolished. In this situation, there is no perceptual constancy of roughness perception at T0. Sectioning of the median nerve abolishes the innervation of the index fingerpad and, consequently, mechanoreceptor signals from the index fingerpad are not transmitted to the brain. Sectioning of the flexor tendons results in a finger flange. This flange environment is not favorable to the propagation of the vibratory waves generated by scanning movements. There is a blockade of afferent

sensation combined with a loss of motor transmission, making roughness imperceptible. Conversely, subjects with an anesthetic ring block of the index finger still have the normal anatomy that enables the propagation of the vibratory waves. That is, they have a selective blockade of afferent sensation only, and in this condition are able to perceive roughness. Moreover, it is important to note that nearly all of the subjects related after the experiment that although they were able to judge roughness with ease while under the influence of the ring block anesthesia, they were unable to perceive any pleasantness from the stimulus. These observations are consistent with the concept of perceptual constancy described by Yoshioka et al. (Yoshioka et al., 2011) and support the notion that signals from different somatosensory submodalities are intermixed as proposed by Saal et al.(Saal and Bensmaïa, 2014).

Our findings indicating that mechanoreceptors in the fingerpad are not the only code-generating anatomical structures that can enable judgment of roughness raise the question of what other structures are involved. Yoshioka et al. [110] and Delhaye et al. (Delhaye et al., 2012) emphasized the role of proprioception. The term proprioception, coined by Sherrington in 1906, refers to the sensory information that underlies one's sense of self-position and movement. While most of the sensory mechanisms underpinning hand-surface interactions are known, information has been lacking about proprioceptors and muscle and joint receptor responses. In an extensive review, Bosco and Poppele [111] proposed a framework of how proprioceptive sensory information seems to be organized as it relates to a sense of body position and movement, but they did not delineate which sensory receptors are involved. Perhaps, some intramuscular receptors (e.g. pressure pain endings, paciniform corpuscles, or stretch receptors; see Introduction) serve additional functions beyond providing the central nervous system with information about muscle length and force.

Brain fMRI studies allow locating brain regions involved in particular tasks, but they do not provide information about the neural codes from the periphery. Dimitriou et al. (Dimitriou and Edin, 2008) developed a paradigm that gives access to neural codes of muscle receptor afferents during unconstrained wrist and digit movements. In their elegant investigations, subjects grasped blocks of different sizes while neural signals from primary and secondary muscle spindle afferents were recorded with microneurography. Further experiments could be performed using this paradigm to

record muscle receptor afferents located in flexor muscles of the index finger during a roughness discrimination task.

4.2- Future investigations

The experiments and results detailed in this thesis had some limitations. Such limitation can lead to the conception of new experimental designs and setups, like those achieved by Delhaye et al (Delhaye et al., 2012). Among the unresolved issues remaining, one merits particular attention. That is, it is unknown why some sensory modalities, such as roughness perception, have "perceptual constancy" in the somatosensory system while others, such as spatial resolution, pressure detection, and temperature detection do not. Specifically, further investigation is needed to elucidate why roughness perception remains intact under digital ring block anesthesia while other forms of sensory perception are completely disrupted.

Regarding the physiology of roughness perception, we would be very interested in conducting an experiment with our roughness discrimination task in patients who have suffered an isolated section of the flexor tendons at the index finger level and comparing their performance before surgical repair versus after recovery from the surgery. Further, we would be intrigued to examine the effect of digital ring block anesthesia on the roughness discrimination ability of such patients. Moreover, neuroimaging studies of subjects with digital ring block anesthesia performing the roughness discrimination task could reveal which brain areas are stimulated in this condition.

These investigations have important implications for the development of technologies that may provide prosthetic hand users with a realistic restoration of sensory feedback systems. Indeed, the development of new prosthetic hand devices with dexterous sensorimotor mechanisms, autonomous functionality, and an acceptable cosmetic appearance is a hot topic in the neurosciences. Initially, prosthetic hand technology was focused on enabling myoelectric control of movements. Myoelectric control is achieved through exploitation of surface electromyographic signals generated by voluntary contractions of residual muscles in the patient's upper extremity. However, with current myoelectric prosthetic hands, it is very difficult for users to control more than one, or at most two, degrees of freedom. Several strategies involving the use of invasive and noninvasive interfaces with the central and peripheral nervous system have been

implemented. Tan et al. (Tan et al., 2014) showed that implanted peripheral nerve interfaces provided stable, natural touch sensation of prosthetic hands for more than a year in two human subjects with upper limb amputations. Electrical stimulation via implanted peripheral nerve cuff electrodes (that did not penetrate the nerve) produced the sensation of touch at multiple locations of the phantom hand with repeatable, stable responses in the two subjects for 16 and 24 months. Unexpectedly, both patients reported that their phantom limb pain had disappeared almost completely since they started using the new prostheses, even when the stimulation was turned off. It is not known if the attenuation of phantom limb pain is due to the re-establishment of naturalistic feedback, the brain re-incorporating the prosthetic hand, or other mechanisms.

In the same way, Raspopovic et al. (Raspopovic et al., 2014) observed that physiologically appropriate (near-natural) sensory information can be provided to an amputee during real-time decoding of grasping tasks to enable the amputee to control a dexterous hand prosthesis. The information is transmitted by stimulating the median and ulnar nerve fascicles (via transversal multichannel intrafascicular electrodes) based on information from sensors in the hand prosthesis. Remarkably, this feedback enabled the participant to modulate the grasping force of the prosthesis with no visual or auditory feedback. Three different force levels were distinguished and used consistently by the subject. Despite these important advances, we are likely many years away from the production of an ideal biomechatronic hand. As summarized by Carrozza et al. (Carrozza et al., 2006), an ideal hand prostheses should fulfill the following requirements:

- In terms of functionality, the device should perform the activities of daily living.
- It should be dexterous and restore motor and motor-related sensory capabilities.
- Finally, it should have a cosmetic appearance that approximates a real hand.

Surveys have indicated that 30–50% of arm amputees do not use their prosthetic hand regularly due primarily to the prosthetics unsatisfactory cosmetic appearance.

To conclude, Delhaye et al. demonstrated that vibrations generated during the scanning of textured surfaces propagate through the finger and hand and stimulate receptor populations in regions far away from the contact region, at least up to the wrist. The spectrum and magnitude of these vibrations should be considered as the best predictors

of roughness discrimination. Therefore, I hope to see the roughness perception problem of prosthetic hands addressed by the development of a prosthetic material designed specifically to produce transmission of the spectrum of vibrations naturally perceived by people with intact hands. Such a material could potentially be placed on the amputation stump to restore roughness perception.

List of figures

Figure 14: Patients with unilateral Carpal Tunnel Syndrome (CTS). (A) Tactile spatial resolution thresholds in TAG scores for unaffected vs. affected hands. (B & C) Just Noticeable Differences (JNDs) in tactile roughness discrimination thresholds with smooth stimuli (B) and rough stimuli (C) in unaffected vs. affected hands. The 75% JNDs are expressed as the absolute difference in the average grit size between a given sandpaper and the reference sandpaper (P320; see Table 1), where LR represents the Limit of Resolution. The line in each graph represents the "identity line".

Figure 15: Patients with a unilateral traumatic sectioning of the median nerve and wrist flexor tendons (TRA-SEC). Just Noticeable Differences (JNDs) in tactile roughness discrimination thresholds with smooth stimuli (left column) and rough stimuli (right column) in unaffected (open circles) vs. affected (black circles) hands. The 75% JNDs are expressed as the absolute difference in the average grit size between a given sandpaper and the reference sans paper (P320; see Table 1), where LR represents the Limit of Resolution. Patients were evaluated four times (except patient 4 who was evaluated three times) during the post-surgical period, i.e., at 1 wk (T0), 3 mos. (T1), between 6 and 9 mos. (T2), and ≥1.5 years (T3).

Figure 16: Subjects with anesthetic ring bloc of the index finger (AN-BLOC). Just Noticeable Differences (JNDs) in tactile roughness discrimination thresholds with smooth stimuli (A) and rough stimuli (B) before and during anesthesia. The 75% JNDs are expressed as the absolute difference in the average grit size between a given sandpaper and the reference sans paper (P320; see Table 1), where LR represents the Limit of Resolution. The line in each graph represents the "identity line".

References

1. Adams, M.J., Johnson, S.A., Lefèvre, P., Lévesque, V., Hayward, V., André, T., Thonnard, J.-L., 2013. Finger pad friction and its role in grip and touch. J R Soc Interface 10, 20120467–20120467.
2. Augurelle, A.S., 2002. Importance of Cutaneous Feedback in Maintaining a Secure Grip During Manipulation of Hand-Held Objects. J Neurophysiol 89, 665–671.
3. Bell-Krotoski, J., Tomancik, E., 1987. The repeatability of testing with Semmes-Weinstein monofilaments. YJHSU 12, 155–161.
4. Bell-Krotoski, J., Weinstein, S., Weinstein, C., 1993. Testing sensibility, including touch-pressure, two-point discrimination, point localization, and vibration. J Hand Ther 6, 114–123.
5. Bell-Krotoski, J.A., Fess, E.E., Figarola, J.H., Hiltz, D., 1995. Threshold detection and Semmes-Weinstein monofilaments. J Hand Ther 8, 155–162.
6. Bensmaïa, S., Hollins, M., 2005. Pacinian representations of fine surface texture. Percept Psychophys 67, 842–854.
7. Bensmaïa, S.J., Hollins, M., 2003. The vibrations of texture. Somatosensory & Motor Res. 20, 33–43.
8. Besne, I., Descombes, C., Breton, L., 2002. Effect of age and anatomical site on density of sensory innervation in human epidermis. Archives of dermatology 138, 1445–1450.
9. Blake, D.T., Hsiao, S.S., Johnson, K.O., 1997a. Neural coding mechanisms in tactile pattern recognition: the relative contributions of slowly and rapidly adapting mechanoreceptors to perceived roughness. J Neurosci 17, 7480–7489.
10. Blake, D.T.D., Johnson, K.O.K., Hsiao, S.S.S., 1997b. Monkey cutaneous SAI and RA responses to raised and depressed scanned patterns: effects of width, height, orientation, and a raised surround. J Neurophysiol 78, 2503–2517.
11. Bleyenheuft, Y., Cols, C., Arnould, C., Thonnard, J.-L., 2006. Age-related changes in tactile spatial resolution from 6 to 16 years old. Somatosensory & Motor Res. 23, 83–87.
12. Bleyenheuft, Y., Thonnard, J.-L., 2007. Tactile spatial resolution measured manually: A validation study. Somatosensory & Motor Res. 24, 111–114.
13. Bolanowski, S.J., Zwislocki, J.J., 1984. Intensity and frequency characteristics of Pacinian corpuscles. I. Action potentials.
14. Brisben, A.J., Hsiao, S.S., Johnson, K.O., 1999. Detection of Vibration Transmitted Through an Object Grasped in the Hand. J Neurophysiol 81, 1548–1558.
15. Brydges, R., Carnahan, H., Dubrowski, A., 2005. Surface exploration using laparoscopic surgical instruments: the perception of surface roughness. Ergonomics 48, 874–894.
16. Buonomano, D.V., Merzenich, M.M., 1998. CORTICAL PLASTICITY: From Synapses to Maps. Annu. Rev. Neurosci. 21, 149–186.
17. Burgess, P.R., Perl, E.R., 1973. Cutaneous Mechanoreceptors and Nociceptors. In: Iggo, A. (Ed.), Handbook of Sensory Physiology. Springer Berlin Heidelberg, pp. 29–78.
18. Carrozza, M.C., Cappiello, G., Micera, S., Edin, B.B., Beccai, L., Cipriani, C., 2006. Design of a cybernetic hand for perception and action. Biological cybernetics 95, 629–644.

19. Cascio, C.J., Sathian, K., 2001. Temporal cues contribute to tactile perception of roughness. Journal of Neuroscience 21, 5289–5296.
20. Chambers, M.R., Andres, K.H., Duering, von, M., Iggo, A., 1972. The structure and function of the slowly adapting type II mechanoreceptor in hairy skin. Quarterly journal of experimental physiology and cognate medical sciences 57, 417–445.
21. Connor, C.E., Hsiao, S.S., Phillips, J.R., Johnson, K.O., 1990. Tactile roughness: neural codes that account for psychophysical magnitude estimates. J Neurosci 10, 3823–3836.
22. Connor, C.E., Johnson, K.O., 1992. Neural coding of tactile texture: comparison of spatial and temporal mechanisms for roughness perception. J Neurosci 12, 3414–3426.
23. Craig, J.C., Johnson, K.O., 2000. The Two-Point Threshold Not a Measure of Tactile Spatial Resolution. Current Directions in Psychological Science 9, 29–32.
24. Delhaye, B., Hayward, V., Lefèvre, P., Thonnard, J.-L., 2012. Texture-induced vibrations in the forearm during tactile exploration. Frontiers in behavioral neuroscience 6, 37.
25. Dellon, A.L., Munger, B.L., 1983. Correlation of histology and sensibility after nerve repair. YJHSU 8, 871–875.
26. Devanandan, M.S., Ghosh, S., John, K.T., 1983. A quantitative study of muscle spindles and tendon organs in some intrinsic muscles of the hand in the bonnet monkey (Macaca radiata). The Anatomical Record 207, 263–266.
27. Dimitriou, M., Edin, B.B., 2008. Discharges in Human Muscle Receptor Afferents during Block Grasping. Journal of Neuroscience 28, 12632–12642.
28. Doucet, Y.S., Woo, S.-H., Ruiz, M.E., Owens, D.M., 2013. The Touch Dome Defines an Epidermal Niche Specialized for Mechanosensory Signaling. CellReports 3, 1759–1765.
29. Fallon, J.B., Macefield, V.G., 2007. Vibration sensitivity of human muscle spindles and Golgi tendon organs. Muscle & nerve 36, 21–29.
30. Gamzu, E., Ahissar, E., 2001. Importance of temporal cues for tactile spatial-frequency discrimination. Journal of Neuroscience 21, 7416–7427.
31. Gerhardt, L.C., Strässle, V., Lenz, A., 2008. Influence of epidermal hydration on the friction of human skin against textiles. Journal of The ….
32. Gescheider, G.A., 1997. Psychophysics: the fundamentals. Psychology Press.
33. Gescheider, G.A., Bolanowski, S.J., Greenfield, T.C., Brunette, K.E., 2005. Perception of the tactile texture of raised-dot patterns: a multidimensional analysis. Somatosensory & Motor Res. 22, 127–140.
34. Giannini, F., Cioni, R., Mondelli, M., Padua, R., Gregori, B., D'Amico, P., Padua, L., 2002. A new clinical scale of carpal tunnel syndrome: validation of the measurement and clinical-neurophysiological assessment. Clinical neurophysiology : official journal of the International Federation of Clinical Neurophysiology 113, 71–77.
35. Gibson, G.O., Craig, J.C., 2002. Relative roles of spatial and intensive cues in the discrimination of spatial tactile stimuli. Percept Psychophys 64, 1095–1107.
36. Goodwin, A.W., Macefield, V.G., Bisley, J.W., 1997. Encoding of object curvature by tactile afferents from human fingers. J Neurophysiol 78, 2881–2888.
37. Gwosdow, A.R., Stevens, J.C., Berglund, L.G., Stolwijk, J.A.J., 1986. Skin Friction and Fabric Sensations in Neutral and Warm Environments. Textile Research Journal 56, 574–580.
38. Halata, Z., Grim, M., Bauman, K.I., 2003. Friedrich Sigmund Merkel and his "Merkel cell," morphology, development, and physiology: review and new results. The anatomical record. Part A, Discoveries in molecular, cellular, and evolutionary biology 271, 225–239.

39. Halata, Z., Munger, B.L., 1980. The sensory innervation of primate eyelid. The Anatomical Record 198, 657–670.
40. Hollins Sliman J Bensmaïa Sean W, M., 2001. Vibrotactile adaptation impairs discrimination of fine, but not coarse, textures. Somatosensory & Motor Res. 18, 253–262.
41. Hollins, M., 2010. Somesthetic senses. Annual review of psychology 61, 243–271.
42. Hollins, M., Bensmaïa, S.J., 2007. The coding of roughness. Canadian Journal of Experimental Psychology/Revue canadienne de psychologie expérimentale 61, 184–195.
43. Hollins, M., Bensmaïa, S.J., Roy, E.A., 2002. Vibrotaction and texture perception. Behav. Brain Res. 135, 51–56.
44. Hollins, M., Risner, S.R., 2000. Evidence for the duplex theory of tactile texture perception. Percept Psychophys 62, 695–705.
45. Hollins, M., Seeger, A., Pelli, G., Taylor, R., 2004. Haptic perception of virtual surfaces: scaling subjective qualities and interstimulus differences. Perception 33, 1001–1019.
46. Hollins, M.M., Faldowski, R.R., Rao, S.S., Young, F.F., 1993. Perceptual dimensions of tactile surface texture: a multidimensional scaling analysis. Percept Psychophys 54, 697–705.
47. Hunt, C.C., 1961. On the nature of vibration receptors in the hind limb of the cat. J Physiol (Lond) 155, 175–186.
48. Hunt, C.C., McIntyre, A.K., 1960a. An analysis of fibre diameter and receptor characteristics of myelinated cutaneous afferent fibres in cat. J Physiol (Lond) 153, 99–112.
49. Hunt, C.C., McIntyre, A.K., 1960b. Characteristics of responses from receptors from the flexor longus digitorum muscle and the adjoining interosseous region of the cat. J Physiol (Lond) 153, 74–87.
50. Hunt, C.C., McIntyre, A.K., 1960c. Properties of cutaneous touch receptors in cat. J Physiol (Lond) 153, 88–98.
51. Johansson, O., Wang, L., Hilliges, M., Liang, Y., 1999. Intraepidermal nerves in human skin: PGP 9.5 immunohistochemistry with special reference to the nerve density in skin from different body regions. J. Peripher. Nerv. Syst. 4, 43–52.
52. Johansson, R.S., Flanagan, J.R., 2009. Coding and use of tactile signals from the fingertips in object manipulation tasks. Nat Rev Neurosci 10, 345–359.
53. Johansson, R.S., Vallbo, Å.B., 1979. Tactile sensibility in the human hand: relative and absolute densities of four types of mechanoreceptive units in glabrous skin. J Physiol 286, 283–300.
54. Johansson, R.S., Westling, G., 1984. Roles of glabrous skin receptors and sensorimotor memory in automatic control of precision grip when lifting rougher or more slippery objects. Exp Brain Res 56, 550–564.
55. Johnson, K.O., 2001. The roles and functions of cutaneous mechanoreceptors. Current Opinion in Neurobiology 11, 455–461.
56. Johnson, K.O., Hsiao, S.S., 1992. Neural Mechanisms of Tactual form and Texture Perception. Annu. Rev. Neurosci. 15, 227–250.
57. Johnson, K.O., Phillips, J.R., 1981. Tactile spatial resolution. I. Two-point discrimination, gap detection, grating resolution, and letter recognition. J Neurophysiol 46, 1177–1192.
58. Johnson, K.O., Yoshioka, T., Vega-Bermudez, F., 2000. Tactile Functions of Mechanoreceptive Afferents Innervating the Hand. Journal of Clinical Neurophysiology 17, 539.

59. Jones, L.A., Lederman, S.J., 2006. Human Hand Function. Oxford University Press.
60. Jozsa, L., Kvist, M., Kannus, P., Jarvinen, M., 1988. The effect of tenotomy and immobilization on muscle spindles and tendon organs of the rat calf muscles. A histochemical and morphometrical study. Acta neuropathologica 76, 465–470.
61. Katz, D., 2013. The World of Touch. Psychology Press.
62. Katz, D., Krueger, L.E., 1989. The world of touch. L. Erlbaum.
63. Klatzky, R.L., Lederman, S.J., 1999. Tactile roughness perception with a rigid link interposed between skin and surface. Percept Psychophys 61, 591–607.
64. Klatzky, R.L., Lederman, S.J., Hamilton, C., Grindley, M., Swendsen, R.H., 2003. Feeling textures through a probe: effects of probe and surface geometry and exploratory factors. Percept Psychophys 65, 613–631.
65. Lauria, G., Holland, N., Hauer, P., Cornblath, D.R., Griffin, J.W., McArthur, J.C., 1999. Epidermal innervation: changes with aging, topographic location, and in sensory neuropathy. Journal of the neurological sciences 164, 172–178.
66. Lederman, S.J., Klatzky, R.L., 1987. Hand movements: a window into haptic object recognition. Cognitive Psychology 19, 342–368.
67. Lederman, S.J., Taylor, M.M., 1972. Fingertip force, surface geometry, and the perception of roughness by active touch. Percept Psychophys 12, 401–408.
68. LIBOUTON, X., Barbier, O., Plaghki, L., Thonnard, J.-L., 2010. Tactile roughness discrimination threshold is unrelated to tactile spatial acuity. Behav. Brain Res. 208, 473–478.
69. Loewenstein, W.R., Skalak, R., 1966. Mechanical transmission in a Pacinian corpuscle. An analysis and a theory. J Physiol (Lond) 182, 346–378.
70. Lucarz, A., Brand, G., 2007. Current considerations about Merkel cells. European Journal of Cell Biology 86, 243–251.
71. M Swash, K.P.F., 1972. Muscle spindle innervation in man. Journal of Anatomy 112, 61.
72. Macefield, V.G., Häger-Ross, C., Johansson, R.S., 1996. Control of grip force during restraint of an object held between finger and thumb: responses of cutaneous afferents from the digits. Exp Brain Res 108, 155–171.
73. Mann, M.D., 1981. The nervous system and behavior. Harpercollins College Division.
74. Maricich, S.M., Morrison, K.M., Mathes, E.L., Brewer, B.M., 2012. Rodents rely on Merkel cells for texture discrimination tasks. Journal of Neuroscience 32, 3296–3300.
75. Maricich, S.M., Wellnitz, S.A., Nelson, A.M., Lesniak, D.R., Gerling, G.J., Lumpkin, E.A., Zoghbi, H.Y., 2009. Merkel Cells Are Essential for Light-Touch Responses. Science (New York, N.Y.) 324, 1580–1582.
76. Mima, T., Ikeda, A., Terada, K., Yazawa, S., Mikuni, N., Kunieda, T., Taki, W., Kimura, J., Shibasaki, H., 1997. Modality-specific organization for cutaneous and proprioceptive sense in human primary sensory cortex studied by chronic epicortical recording. Electroencephalography and Clinical Neurophysiology/Evoked Potentials Section 104, 103–107.
77. Moore, T.J., 1970. A Survey of the Mechanical Characteristics of Skin and Tissue in Response to Vibratory Stimulation. Man-Machine Systems, IEEE Transactions on 11, 79–84.
78. Morley, J.W., Hawken, M.J., Burge, P.D., 1988. Vibratory detection thresholds following a digital nerve lesion. Exp Brain Res 72, 215–218.
79. Mountcastle, V.B., 2005. The Sensory Hand. Harvard University Press.
80. Mountcastle, V.B., n.d. The sensory hand: neural mechanisms of somatic sensations.
81. Munger, B.L., Ide, C., 1988. The structure and function of cutaneous sensory receptors. Archives of histology and cytology 51, 1–34.

82. Nelson, R.J., 2010. The Somatosensory System: Deciphering the Brain's Own Body Image.
83. Olausson, H., Lamarre, Y., Backlund, H., Morin, C., Wallin, B.G., Starck, G., Ekholm, S., Strigo, I., Worsley, K., Vallbo, Å.B., Bushnell, M.C., 2002. Unmyelinated tactile afferents signal touch and project to insular cortex. Nat Neurosci 5, 900–904.
84. Par, M., Behets, C., Cornu, O., 2003. Paucity of presumptive ruffini corpuscles in the index finger pad of humans. The Journal of Comparative Neurology 456, 260–266.
85. Practice parameter for carpal tunnel syndrome (summary statement). Report of the Quality Standards Subcommittee of the American Academy of Neurology, 1993. Practice parameter for carpal tunnel syndrome (summary statement). Report of the Quality Standards Subcommittee of the American Academy of Neurology. Neurology 43, 2406–2409.
86. Randolph, M., Semmes, J., 1974. Behavioral consequences of selective subtotal ablations in the postcentral gyrus ofMacaca mulatta. Brain Res 70, 55–70.
87. Raspopovic, S., Capogrosso, M., Petrini, F.M., Bonizzato, M., Rigosa, J., Di Pino, G., Carpaneto, J., Controzzi, M., Boretius, T., Fernandez, E., Granata, G., Oddo, C.M., Citi, L., Ciancio, A.L., Cipriani, C., Carrozza, M.C., Jensen, W., Guglielmelli, E., Stieglitz, T., Rossini, P.M., Micera, S., 2014. Restoring natural sensory feedback in real-time bidirectional hand prostheses. Science translational medicine 6, 222ra19.
88. Saal, H.P., Bensmaïa, S.J., 2014. Touch is a team effort: interplay of submodalities in cutaneous sensibility. Trends in Neurosciences 1–9.
89. Sathian, K., Goodwin, A.W., John, K.T., Darian-Smith, I., 1989. Perceived roughness of a grating: correlation with responses of mechanoreceptive afferents innervating the monkey's fingerpad. J Neurosci 9, 1273–1279.
90. Sathian, K., Zangaladze, A., 1996. Tactile spatial acuity at the human fingertip and lip: bilateral symmetry and interdigit variability. Neurology 46, 1464–1466.
91. Sathian, K., Zangaladze, A., Green, J., Vitek, J.L., DeLong, M.R., 1997. Tactile spatial acuity and roughness discrimination: impairments due to aging and Parkinson's disease. Neurology 49, 168–177.
92. Scheibert, J., Leurent, S., Prevost, A., Debregeas, G., 2009. The Role of Fingerprints in the Coding of Tactile Information Probed with a Biomimetic Sensor. Science 323, 1503–1506.
93. Skedung, L., Danerlöv, K., Olofsson, U., Aikala, M., Niemi, K., Kettle, J., Rutland, M.W., 2010. Finger Friction Measurements on Coated and Uncoated Printing Papers. Tribol Lett 37, 389–399.
94. Smith, A.M., Basile, G., Theriault-Groom, J., Fortier-Poisson, P., Campion, G., Hayward, V., 2010. Roughness of simulated surfaces examined with a haptic tool: effects of spatial period, friction, and resistance amplitude. Experimental brain research Experimentelle Hirnforschung Expérimentation cérébrale 202, 33–43.
95. Smith, A.M., Chapman, C.E., Deslandes, M., Langlais, J.-S., Thibodeau, M.-P., 2002. Role of friction and tangential force variation in the subjective scaling of tactile roughness. Exp Brain Res 144, 211–223.
96. Srinivasan, M.A., Whitehouse, J.M., LaMotte, R.H., 1990. Tactile detection of slip: surface microgeometry and peripheral neural codes. J Neurophysiol 63, 1323–1332.
97. Tabot, G.A., Dammann, J.F., Berg, J.A., Tenore, F.V., Boback, J.L., Vogelstein, R.J., Bensmaïa, S.J., 2013. Restoring the sense of touch with a prosthetic hand through a brain interface. Proceedings of the National Academy of Sciences of the United States of America.
98. Takahashi-Iwanaga, H., Abe, K., 2001. Scanning electron microscopic observation of Merkel cells in the lamprey epidermis. Kaibogaku zasshi. Journal of anatomy 76, 375–

380.
99. Tan, D.W., Schiefer, M.A., Keith, M.W., Anderson, J.R., Tyler, J., Tyler, D.J., 2014. A neural interface provides long-term stable natural touch perception. Science translational medicine 6, 257ra138.
100. Taylor, M.M., Lederman, S.J., 1975. Tactile roughness of grooved surfaces: A model and the effect of friction. Percept Psychophys 17, 23–36.
101. Tremblay, F., Wong, K., Sanderson, R., Coté, L., 2003. Tactile spatial acuity in elderly persons: assessment with grating domes and relationship with manual dexterity. Somatosensory & Motor Res. 20, 127–132.
102. Trulsson, M., Francis, S.T., Kelly, E.F., Westling, G., Bowtell, R., McGlone, F., 2001. Cortical responses to single mechanoreceptive afferent microstimulation revealed with fMRI. Neuroimage 13, 613–622.
103. Turnbull, B.G., Rasmusson, D.D., 1986. Sensory Innervation of the Raccoon Forepaw: 1. Receptor Types in Glabrous and Hairy Skin and Deep Tissue. Somatosensory & Motor Res. 4, 43–62.
104. Vallbo, Å.B., Hagbarth, K.E., 1968. Activity from skin mechanoreceptors recorded percutaneously in awake human subjects. Exp. Neurol. 21, 270–289.
105. Vallbo, Å.B., Johansson, R.S., 1984. Properties of cutaneous mechanoreceptors in the human hand related to touch sensation. Hum Neurobiol 3, 3–14.
106. Van Boven, R.W., Hamilton, R.H., Kauffman, T., Keenan, J.P., Pascual-Leone, A., 2000. Tactile spatial resolution in blind braille readers. Neurology 54, 2230–2236.
107. Van Boven, R.W., Johnson, K.O., 1994a. The limit of tactile spatial resolution in humans: grating orientation discrimination at the lip, tongue, and finger. Neurology 44, 2361–2366.
108. Van Boven, R.W., Johnson, K.O., 1994b. A psychophysical study of the mechanisms of sensory recovery following nerve injury in humans. Brain 117 (Pt 1), 149–167.
109. Vega-Bermudez, F., Johnson, K.O., 2004. Fingertip skin conformance accounts, in part, for differences in tactile spatial acuity in young subjects, but not for the decline in spatial acuity with aging. Percept Psychophys 66, 60–67.
110. Voss, H., 1971. Voss: Tabelle der absoluten und relativen Muskelspindelza... - Google Scholar. Anat Anz.
111. Werner, R.A., Andary, M., 2002. Carpal tunnel syndrome: pathophysiology and clinical neurophysiology. Clinical neurophysiology : official journal of the International Federation of Clinical Neurophysiology 113, 1373–1381.
112. Wilkinson, K.D., Lee, K.M., Deshpande, S., Duerksen-Hughes, P., Boss, J.M., Pohl, J., 1989. The neuron-specific protein PGP 9.5 is a ubiquitin carboxyl-terminal hydrolase. Science (New York, N.Y.) 246, 670–673.
113. Yoshioka, T., Bensmaïa, S.J., Craig, J.C., Hsiao, S.S., 2007. Texture perception through direct and indirect touch: An analysis of perceptual space for tactile textures in two modes of exploration. Somatosensory & Motor Res. 24, 53–70.
114. Yoshioka, T., Craig, J.C., Beck, G.C., Hsiao, S.S., 2011. Perceptual constancy of texture roughness in the tactile system. Journal of Neuroscience 31, 17603–17611.
115. Yoshioka, T., Gibb, B., Dorsch, A.K., Hsiao, S.S., Johnson, K.O., 2001. Neural coding mechanisms underlying perceived roughness of finely textured surfaces. Journal of Neuroscience 21, 6905–6916.
116. Young, B.P.D., 2006. Wheater's Functional Histology.
117. Zwislocki, J.J., 2001. On a psychophysical transformed-rule up and down method converging on a 75% level of correct responses. Proceedings of the National Academy of Sciences 98, 4811–4814.